Received: 31 January 2022 | Revised: 12 May 2022 | Accepted: 15 May 2022

DOI: 10.1002/gj.4514

SPECIAL ISSUE ARTICLE

WILEY

Basement cross-strike Bomdila Fault beneath Arunachal Himalaya: Deformation along curved thrust traces, seismicity, and implications in hydrocarbon prospect of the Gondwana sediments

Tapos Kumar Goswami[1] | Pranjit Kalita[1] | Soumyajit Mukherjee[2] | Bashab Nandan Mahanta[3] | Ranjan Kumar Sarmah[1] | Ramesh Laishram[3] | Hiruj Saikia[3] | Mousumi Gogoi[1] | Ratamali Machahary[1] | Bhaskar Oza[4]

[1]Department of Applied Geology, Dibrugarh University, Dibrugarh, India

[2]Department of Earth Sciences, Indian Institute of Technology Bombay, Mumbai, India

[3]Regional Headquarters, NER, Geological Survey of India, Shillong, India

[4]State Unit: Arunachal Pradesh, Geological Survey of India, Itanagar, India

Correspondence
Soumyajit Mukherjee, Department of Earth Sciences, Indian Institute of Technology Bombay, Powai, Mumbai 400 076, Maharashtra, India.
Email: soumyajitm@gmail.com; smukherjee@iitb.ac.in

Funding information
IIT Bombay; CPDA grant; International Geological Congress Secretariat, New Delhi (IGC-2020), Grant/Award Number: NER-001

Handling Editor: A. K. Singh

Structural mapping and fieldwork in the Lesser and Higher Himalayan sequences in the western Arunachal Himalaya reveal crucial deformation fabrics in the Main Central Thrust (MCT) and Dirang Thrust (DT) zones. The top-to-SW ductile shear in the MCT and DT zones is correlated with the swing in the trend of MCT and DT from NE to NNW. The curved MCT and DT as traced by previous authors on the regional map of Arunachal Himalaya are studied. It is found that at places where these faults swing, shear senses developed at the meso-scale. These shear senses are studied in meso- and micro-scales. Seismicity in the western Arunachal Himalaya is influenced by basement cross-strike crustal-scale NW-trending buried Bomdila Fault (BF). Landslides occur frequently along the Bhalukpong-Bomdila–Sela traverse are also linked with the transverse BF. In its southern part, the BF coincides with the Dhansiri Lineament and is the basin margin fault in the upper Assam shelf. The Gondwana sediments extended further south below the Brahmaputra alluvium along the fault is to be explored for hydrocarbon exploration.

KEYWORDS
Bomdila Fault, Gondwana sediments, hydrocarbon prospect, seismotectonics

1 | INTRODUCTION

The Himalayan mountain chain was developed by the collision between the Indian and the Eurasian plates since ~55 Ma (Hodges, 2000; Hu et al., 2016). The arcuate length of the Himalayan fold-thrust belt stretches for ~2,400 km from the western to the eastern syntaxis (DeCelles, Robinson, & Zandt, 2002). India-Eurasia collision led to triclinic transpression at the plate to plate contact (Duta & Mukherjee, 2021).The collision between the two plates has been accommodated by a number of north-dipping major thrusts. The crustal shortening is thus concentrated in these major thrusts in the south of the extensional zone known as the South Tibet Detachment Zone (Kellett, Cottle, & Larson, 2018). The crustal-scale fault imbrications produced due to collision developed four major tectonic units. Towards the south, these are: (a) Tethyan Himalaya, (b) Higher Himalaya (c) Lesser Himalaya, consisting of two parts—a crystalline and a sedimentary sequence, and (d) Sub-Himalaya/Siwalik Hills (Heim & Gansser, 1939). These tectonic zones are separated from each other by three major south-vergent thrusts: (a) Main Central Thrust (MCT) occurring as a fault zone (b) Main Boundary Thrust (MBT), and the (c) Main Frontal Thrust (MFT) (Le Fort, 1975) (Figure 1). One of the major crustal-scale thrusts in the Himalaya is the MCT, along which the high-grade metamorphic Higher Himalayan Crystallines (HHC) is thrust over the low-grade Lesser Himalayan

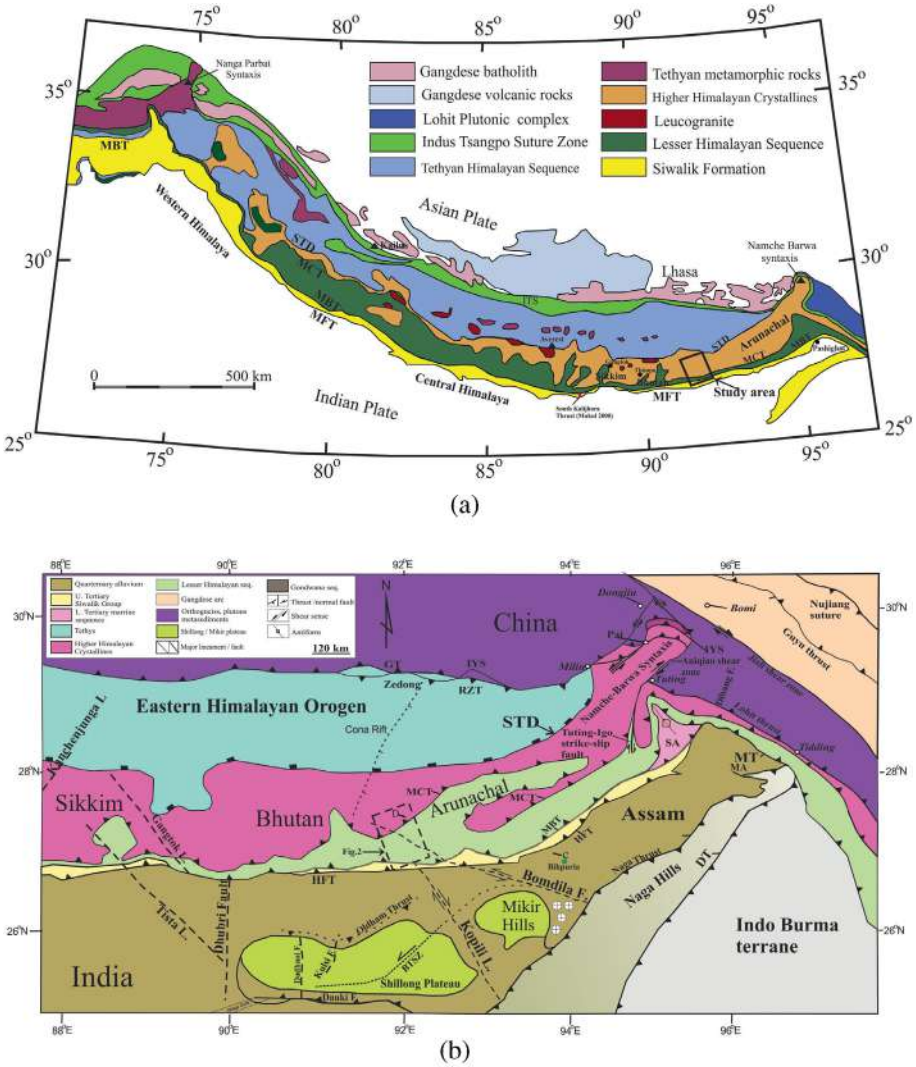

FIGURE 1 (a) Geologic map of the Himalayan orogen (modified from Zhang, Xiang, Dong, Ding, & he, Z., 2015) showing the location of Arunachal Himalaya. The study area is shown within the rectangle. (b) Regional geological sketch map of eastern Himalaya, Namche Barwa Syntaxis and adjoining regions (modified from Ding, Zhong, Yin, Kapp, & Harrison, 2001). The study area is within the bold rectangle. Kanchenjunga, Tista, Gangtok, Dhubri, Kopili and Bomdila faults are shown (Dasgupta et al., 2013; Kayal et al., 2012). The location of oil fields (solid white circles with cross) in the south-west of Bomdila Fault and Bihpuria well (solid green circle) are shown. DT, Disang Thrust; GT, Gangdese Thrust; HFT, Himalayan Frontal Thrust; IYS, Indus Yalu Suture; MA, Manabhum Anticline; MBT, Main Boundary Thrust; MCT, Main Central Thrust; MT, Mishmi Thrust; NT, Naga Thrust; RZT, Renbu Zedong Thrust; SA, Siang Antiform; STD, South Tibet Detachment

rocks (Gansser, 1964; Martin, 2016). Thrusting along the MCT occurred throughout the Himalayan orogen during the late Oligo-early Miocene, and the crystalline rocks were emplaced over the Lesser Himalaya, such as Pandoh-Jutogh in Himachal, Baijnath-Almora in Kumaun, Dudalhera-Kathmandu in Nepal, Shumar in Bhutan, and Bomdila in western Arunachal Pradesh (Bikramaditya, Sen, & Sangode, 2017; Patel, Singh, & Lal, 2015; Singh et al., 2022; Singh & Patel, 2017, 2022; Singh, Patel, & Chaudhary, 2022; Singh, Patel, & Lal, 2012; Singh & Singhal, 2020). In the western Arunachal Himalaya (India), the Lesser Himalayan Crystallines (LHC), in the north of Bome Thrust (Yin et al., 2010b), are divided into two units. The lower unit (basal LHC) is dominated by mylonitic Bomdila Gneiss (BG), phyllites and quartzites, and the upper unit (upper LHC) consists of the schistose rocks of the Dirang Formation (DF). The lower unit of the LHC is juxtaposed against the upper unit along the Dirang Thrust (DT) (Bikramaditya & Gururajan, 2011; Goswami, Bezbaruah, Mukherjee, Sarmah, & Jabeed, 2018; Goswami, Mahanta, Mukherjee, Syngai, & Sarmah, 2020). The MCT marks significant variation in structural geometry along its length (Biswal, 1997; Singh & Thakur, 2001). A recent review on tectonics of eastern Himalaya can be found in the recent special volume (Singh, Chung, & Somerville, 2022) in the *Geological Journal*.

In Himalaya, along-strike variation in the deformation style, crustal shortening, and seismicity are well established (Dasgupta, Mukhopadhyay, & Mukhopadhyay, 2013; Duvall, Waldron, Godin, & Najman, 2020; Mukherjee, 2013; Rajendran, Parameswaran, & Rajendran, 2017; Yin, 2006). The arcuate shape of the orogen and the great earthquake rupture zones are connected to transverse fractures and faults on the subducting Indian basement (Gahalaut & Kundu, 2012). Therefore, our understanding of the configuration of the colliding Indian basement and its influence in building the Himalayan architecture needs more clarity. The Himalayan thrusts as MFT, MBT, and MCT are affected by the basement transverse faults and this can be studied through outcrop- scale deformational imprints in the thrust zones. The inherited structures in the Indian basement might have influenced the Himalayan orogen during the entire span of subduction and collision. There are palaeo-topographic ridges in the Indian basement, which are connected to orogen-perpendicular faults. The Himalayan orogen from west to east is segmented by these transverse faults (Godin & Harris, 2014 and references therein). Along-

strike variation of seismicity is attributed to segmentation of the Main Himalayan Thrust (e.g., Pandey, Tandukar, Avouac, Vergne, & Heritier, 1999). Geomorphic evidences like mountain front advancement or change of the river courses are associated with upper crustal faults. These faults are connected to basement ridges that extends beneath the Himalayan orogen (e.g., Bose & Mukherjee, 2019; Goswami, Bhowmik, Dasgupta, & Pant, 2014).

Despite the lack of deep seismic data, the basement structures are presumed to extend towards the north below the Himalaya (Gahalaut & Kundu, 2012). Large earthquakes along the leading part of the Main Himalayan Thrust (MHT) ruptured the surface. In western Bhutan, the geometry of MHT especially in the northern part represents an interseismic stress build–up and poses a greater seismogenic potential (Diehl et al., 2017; Zhao et al., 2021). This part is intersected by basement cross-strike Kopili Fault.

In the Arunachal Himalaya, the Proterozoic rocks of the Lesser Himalayan Sequences (LHS) crop out in a vast track from the western to the eastern part. The complexity in the deformation style in the LHS is inadequately constrained along the orogenic trend (Goswami, Mahanta, et al., 2020; Singh & Chowdhury, 1990; Srivastava, Srivastava, Srivastava, & Singh, 2011). The present study discusses the deformation in the LHS from the Dedza-Sela sector in western Arunachal Pradesh.

This work also aims to investigate the deformation kinematics in the MCT and DT zones through meso- to micro-scale ductile to ductile-brittle fabrics imprinted in the rocks. We highlight the influence of the basement cross-strike faults in the orientation of the major Himalayan thrusts such as the MCT in Arunachal Himalaya. Finally, the hydrocarbon potential of Gondwana sediments in the Upper Assam shelf is discussed from a cross-section in the east of the Bomdila Fault.

Reactivation of basement structures in the orogen is documented from a number of studies (Godin, Roche, Waffle, & Harris, 2018; Thomas, 2006 and references therein). The configuration of the Indian basement is very crucial for understanding the seismicity along the strike of the Himalayan orogen. For example, deep-seated basement structures (e.g., Tista, Gangtok, and Kopili faults) may be the cause for the variation in the (a) ductile strain (Gibson, Godin, Kellett, Cottle, & Archibald, 2016), (b) exhumation rate (Yin & Harrison, 2000) and (c) seismicity (Gahalaut & Kundu, 2012; Mugnier et al., 2017) along the strike of the Himalaya. In eastern India, the Eocene Hinge Zone (see south of Dhubri Fault in Figure 1b), that separates the Bengal Basin in the NW and the oceanic crust in the SE, align with the Dhubri Fault in the west of the Shillong Plateau (Curray, 2014; Godin et al., 2018; Godin & Harris, 2014) (Figure 1b). In the eastern Himalaya, a cluster of seismic epicentral plots constrain the continuation of the basement fault in the Himalayan mountain belt. Many earthquakes located in the footwall of the MHT yield strike-slip focal mechanism for transverse faults in the Himalaya (Dasgupta, Mukhopadhyay, & Nandy, 1987; Kayal, 2001; Kayal et al., 2010; M. Mukhopadhyay, 1984a; S. C. Mukhopadhyay, 1984b). The 2011 Darjeeling earthquake (Mw 6.9) related strike-slip reactivation of the Tista lineament is speculated to be genetically linked to the Munger-Saharsa ridge (Diehl et al., 2017; Ni & Barazangi, 1984; Pradhan et al., 2013). The Pingla and the Kishanganj Faults mark the eastern edge of the Munger-Saharsa Ridge. The Kishanganj Fault is an active basement fault in the Himalayan belt and extends through Sikkim to the Tibetan Plateau offsetting the South Tibetan Detachment (Rao et al., 2015).

In the Shillong Plateau, the Dudhnoi, Kulsi and the Krishnai faults are oriented ~N–S and are transverse to the Himalayan arc (Figure 1b). However, there is no information on the continuation of these faults below the Himalayan orogen. Regionally extensive faults or lineaments like Kanchenjunga, Tista, Gangtok lineaments and the Dhubri Fault have produced prominent offsets of MFT, MBT, or MCT in the eastern Himalaya. The offsets in the MCT, MBT, and MFT in the map-scale are due to the orogen-transverse lineaments, for example, the Tista, Gangtok and Kopili lineaments (Figure 1b).

In other parts of the Himalaya, the manifestations of the interactions of the ridges and subduction arc in the form of 'concave outward local cusp' involving MFT and MBT are observed (Bollinger et al., 2004; Gahalaut & Kundu, 2012). For example, the Faizabad Ridge makes a cusp or dent in the MFT; similarly, the Munger-Saharsa ridge interacts with MFT and forms a cusp. Bends/salients of MCT in Sikkim and Bhutan might have formed due to the cross-strike Tista and Kopili Faults in the underthrust Indian basement (Dasgupta et al., 2013; De & Kayal, 2004; Kayal et al., 2010, 2012; Mitra, Bhattacharyya, & Mukul, 2010) (Figure 1b). The field evidence for salients in the MCT is observed in the form of ductile shear fabrics in the thrust zones depicting a consistent top-to-SW shear. The Kopili Fault has been seismically active (two major quakes Mw 6.3 and 5.1 in September, 2009 and Mw 6.4 earthquake in April, 2021) (Nandy, 2001; Kayal et al., 2010, 2012; Baruah & Kayal, 2013; Panthi, Singh, & Shankar, 2013; Sharma, Sarma, & Baruah, 2018).

The strike-slip NE-dipping Bomdila Fault in the east of Kopili Fault is a basement fault, which runs in WNW–ESE trend from the Belt of Schuppen to the MCT (Figure 1b). Two major rivers in the Brahmaputra valley, Dhansiri and Bargang, follow straight courses parallel to the trend of the Bomdila Fault (i.e., ~NW–SE) (Sarma & Sharma, 2018; Sharma et al., 2018). In the NW part, the salient (curved trace in the MCT—concave to the foreland) in the MCT might be due to the Bomdila Fault. The evidence for this is the sudden swing in the trace of the MCT from NE–SW to NW–SE in the map-scale. Further, the NW–SE trace of the MCT is parallel to the C-plane with top-to-SSE shear in the footwall sequence of the Bomdila Gneisses. The salient in the MCT is well observed in the map-scale (Figures 1 and 2a,d). The trend of MCT and DT swings from ENE–WSW to NE–SW in the map scale. Field documentation of the ductile shear fabrics indicates: (a) top-to-SW sense of shear, both in the MCT and DT zones, is parallel to the NE–SW trend of MCT and DT, and (b) the mylonitic Bomdila Gneisses show a top-to-SE sense of ductile shear (C-plane) which is parallel to the NW–SE trend of MCT and DT (MCT and DT zones are shown clearly in the structural map. Coordinates are given in the structural map in the 5′ interval). It is worth noting that the trend of MCT and DT again follows an ENE–WSW trend to the west of the salients as observed in the map-scale (Figure 2).

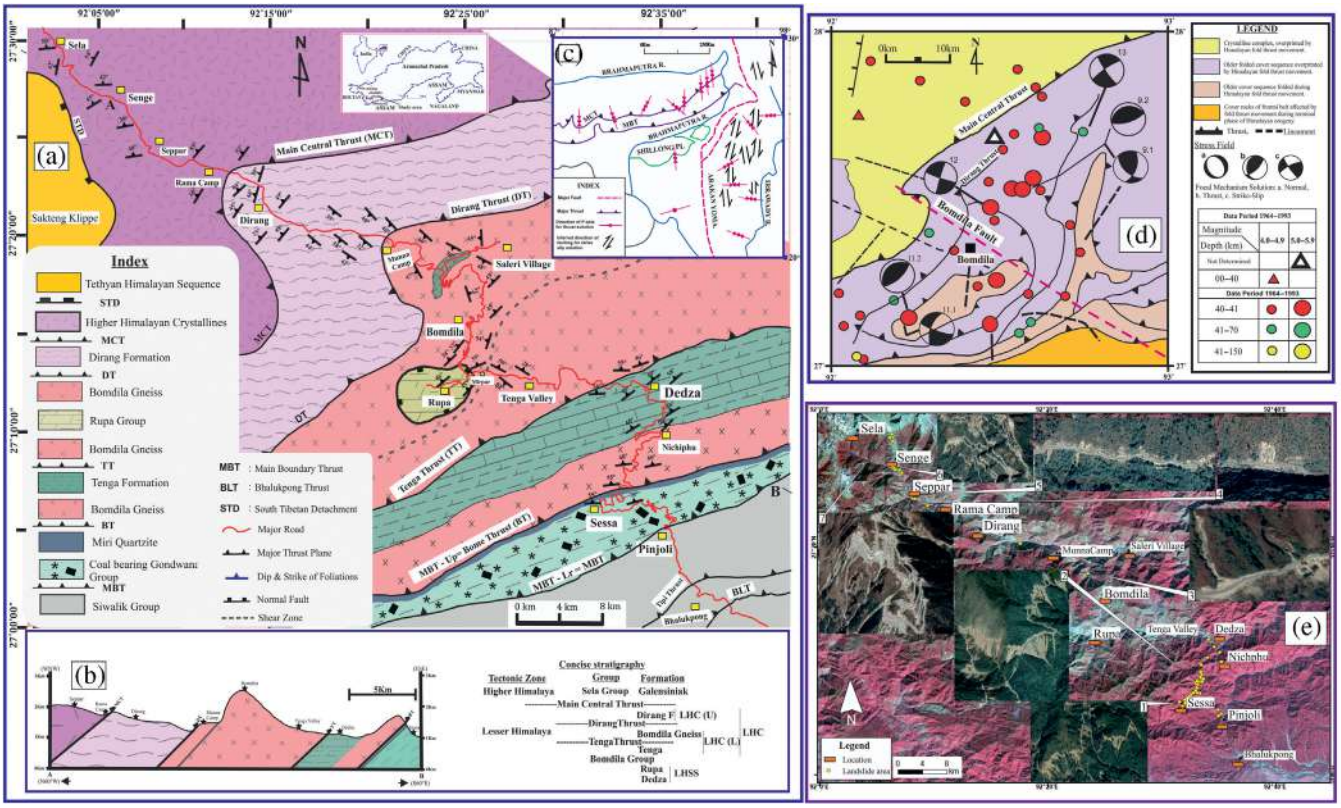

FIGURE 2 (a) Geological map of the western Arunachal Pradesh. In addition to the data from this study, the map incorporates elements from Yin et al. (2010a) and DeCelles et al. (2016) (inset: Location map of the area studied). The continuity of the Miri Formation quartzite (in the footwall of Bome Thrust) is shown through field data from this study and DeCelles et al. (2016). (b) Section along AB is shown. The concise stratigraphy of the area is incorporated. The Gondwana sequence in the footwall of the Bome Thrust is shown. (c) The compression axis map (modified from Verma, 1985) for western Arunachal Pradesh. The NNW–SSE compression is depicted for western Arunachal segment. (d) The seismotectonic map for the western Arunachal Pradesh (modified from Seismotectonic atlas, GSI, 2000). The salient in the MCT and DT and WNW trending Bomdila Fault is shown. Inset—earthquakes associated with Bomdila Fault during 1964–1993. Events showing strike-slip FMS during 1984–2015 as per Sharma et al. (2018). (e) Landslide map along Balukpong-Bomdila–Sela section of Arunachal Pradesh (prepared by us). Numbers of earthquakes in different locations shown from Pinjoli to Sela

The Bomdila Fault in the western Arunachal Himalaya trends WNW–ESE, which runs from belt of schuppen in the SE to NW of MCT. The focal mechanism solution indicates that the fault is strike-slip with left-lateral shear (Sarma & Sharma, 2018). The fault is seismogenic and the northern part of the fault is more active than the southern part (Sharma et al., 2018). There are geomorphologic evidences that Dhansiri and Bargang rivers follow a straight course parallel to the ~NW–SE Bomdila Fault (Sarma & Sharma, 2018; Sharma et al., 2018).

Ductile deformation of the MCT hangingwall and footwall sequences in the western Arunachal Himalaya have not been studied adequately (Bhattacharya & Nandy, 2007; Bikramaditya & Gururajan, 2011; Sarma, Bhattacharyya, Nandy, Konwar, & Mazumdar, 2014; Srivastava et al., 2011). How the buried basement faults affect the major Himalayan thrusts, for example, MCT and MBT has remained indeterminate. Further, the changing pattern of the mesoscopic ductile deformation in the MCT zone or in the MCT footwall have not been constrained so far.

2 | METHODOLOGY

Mapping was done on a toposheet with a scale of 1:50,000 from Pinjoli to Sela. For convenience, the entire traverse was divided into three segments (Section 3). Samples are collected from the LHS and HHC across the MCT and DT. Oriented samples are collected for the preparation of thin sections from the hangingwall and footwall sequences of MCT and DT. Orientations of the structural elements of different generations of deformation in the LHS and HHC are recorded in the field.

3 | GEOLOGY

The study area is located in the West Kameng District of Arunachal Pradesh of NE Himalaya (Table 1 presents the stratigraphy). The HHC in the MCT hangingwall consists of kyanite-bearing migmatitic gneisses and orthogneisses of Neoproterozoic to Ordovician age

(DeCelles, Carrapa, Gehrels, Chakraborty, & Ghosh, 2016; Yin et al., 2010a). The DT brings the Mesoproterozoic Lesser Himalayan Crystallines (LHC) of the Dirang Formation (DF) over the Palaeoproterozoic Bomdila Gneisses (BG) (DeCelles et al., 2016; Goswami et al., 2014). The Dirang Formation (DF) is equivalent to the Jaishidanda Formation of Bhutan (Daniel, Hollister, Parrish, & Grujic, 2003; DeCelles et al., 2016). However, rocks of the DF are also interpreted as either low-grade protolith of the HHC or high-grade LHS rocks (DeCelles et al., 2016; Yin, 2006).

The LHC is further divided into a lower unit consisting of mylonitic Bomdila Gneiss (BG) and Salari Granite with garnet-mica schists and amphibolites and an upper unit composed of garnet-kyanite -staurolite-schist, quartzites and phyllites. Dirang Thrust (DT) separates these two units (Figure 2). Bomdila Gneiss yielded whole-rock Rb-Sr isochron ages, which range between 1,914 ± 23 Ma (Dikshitulu, Pandey, Krishna, & Raju, 1995) and 207Pb/206Pb age of 1,752 ± 23 Ma (Pathak & Kumar, 2019), while high-Ca Salari granite yielded an Rb–Sr age of 1,528 ± 60 Ma (Dikshitulu et al., 1995) and U–Pb ages between 1,791 and 1,768 Ma (Bikramaditya, Chung, Singh, Lee, & Lemba, 2021).

The metapelitic sequence of the LHC was intruded by the Bomdila Gneisses (BG) in the hangingwall of the Bome Thrust in the SE. In the NW of Bomdila, Dirang Formation was thrust over the Bomdila Gneisses along the Dirang Thrust. Thus, there are repeated occurrences of the mylonitic augen Bomdila orthogneisses along the studied section. Ductile shear fabrics are better developed in BG in its marginal parts (along the thrust contacts with Tenga and Dirang Formation) than its interior. The asymmetric porphyroclasts and the mylonitic S-C fabrics in BG display a consistent top-to-SE shear.

The DF mainly consists of garnet-muscovite-biotite schists, quartzites, phyllites, calc-silicates, and minor amphibolite bands. The gradual increase of the metamorphic grade of the rocks of the DF from Munna-Camp towards MCT is observed with the appearance of kyanite and staurolite in association with garnet, biotite, and muscovite (Bhattacharyya & Nandy, 2007; Goswami, Bhowmik, & Dasgupta, 2009). Towards MCT, the pelitic schists of the Dirang Formation shows occasionally kyanite and staurolites in addition to garnet, biotite, and muscovite (Bhattacharyya & Nandy, 2008; Goswami et al., 2009). Frequency of mylonitic foliation, conjugate shear bands, and orthogniesses inter-layered with leucogranite sills and veins indicate deformation of the footwall sequences close to the MCT (Saha, 2013; Saha, Sengupta, & Das, 2011).

TABLE 1 Generalized tectonostratigraphic succession of the West Kameng District, Arunachal Pradesh (modified after Das, Bakliwal, & Dhoundial, 1975; Kumar, 1997; Bhattacharjee & Nandy, 2007; Goswami et al., 2009)

Tectonic Zones	Groups	Formations	Lithology
Higher Himalaya	SELA GROUP	Galensiniak Formation	Migmatite, garnetiferous Bt-Pl gneiss, calc-gneiss/marble, staurolite schist, tourmaline-bearing leucogranite, quartzite and pegmatite.
		Taliha Formation	Not exposed
~~Main Central Thrust (MCT)~~~~~~~~~~~~~~~~~~~~			
LESSER HIMALAYA	DIRANG (Upper Unit)		Garnetiferous Ms-Bt schist, phyllite, sericite quartzite, calc-silicate and Tr-Act marble.
	~~Dirang Thrust (DT) ~~~~~~~~~~~~~~~~~~~~		
	BOMDILA GROUP	Bomdila Gneiss (Lower Unit) LHC	Mylonitic augen gneiss, granite, amphibolite.
		~~Tenga Thrust (TT)~~~~~~~~~~~~~~~~~~~~	
		Tenga (Lower Unit)	Quartzite, phyllites, schist, micaceous sandstone.
		Rupa and Dedza (**LHSS**)	Dolomite, quartzite, carbonaceous phyllite.
	~~Main Boundary Thrust- Upper = Bome Thrust (BT)~~~~~~~~~~~~~~~~~~		
	GONDWANA GROUP		Carbonaceous shale, sandstone with coal bands and slate.
~~Main Boundary Thrust-Lower (MBT)~~~~~~~~~~~~~~~~~~~			
SUB-HIMALAYA	SIWALIK GROUP	Dafla Formation	Grey to green sandstone.
		~~Tipi Thrust~~~~~~~~~~~~~	
		Subansiri Formation	Siltstone with salt-pepper texture.
		~~Bhalukpong Thrust~~~~~~~~~~~~~	
		Kimin Formation	Pebble to boulder bed.
~~Himalayan Frontal Thrust (HFT)~~~~~~~~~~~~~~~~~			

In the north of Seppar, garnet and kyanite-bearing migmatites, biotite-plagioclase gneiss, staurolite schists, calc-gneiss or marble bands, tourmaline-bearing leucogranites, and quartzites of the Sela Group differentiates the footwall sequences of DF in the south of the Rama Camp (Bhattacharyya & Nandy, 2007; Srivastava et al., 2011).

3.1 | Field input

We mapped the area in three NW-SE traverses: (a) Pinjoli–Bomdila transect, (b) Bomdila-Dirang transect and (c) Dirang-Sela transect (Figure 2). The length of these transects are: 86 km (Pinjoli-Bomdila), 42 km (Bomdila-Dirang) and 62 km (Dirang-Sela). Based on our field data and in the combination with the existing information we have prepared the geological map of the area in the scale of 1:50,000 (Figure 2). The thrust contact between the BG and the Mesoproterozoic DF is shown as DT on the basis of our field data and the existing one by Bikramaditya, Sen & Sangode, (2017). The DT shown in the present study may be a continuation of the East Dirang Thrust (EDT) mapped by DeCelles et al. (2016). We have mapped a ductile shear zone in the Bomdila Gneisses around Mirpur (27°12′48″N:92°25′11.8″E) (Figures 2 and 3). We documented ~200 m thick NE–SW trending ductile sheared MCT zone near Seppar (Figure 3), where the meso-scale kinematic indicators in garnet-bearing schists indicate top-to-SW shear. The DT was traced for ~1 km near Munna Camp in the West Kameng District of Arunachal Pradesh based on the abundance of mylonitic foliation, increase in grain size, the appearance of garnet, staurolite, and micas in the rocks of the DF. The MCT was mapped (~16 km NW of Dirang) based on: (a) frequency of mylonitic foliations, (b) appearances of orthogneisses interlayered with sills and veins of leucogranites, and (c) first appearance of kyanites in the pelitic schists of the DF. In the footwall of the BT, the Miri Quartzite is shown as a mappable unit (Figures 2 and 3). Figures 2 and 3 present the lithology and structural elements in the area.

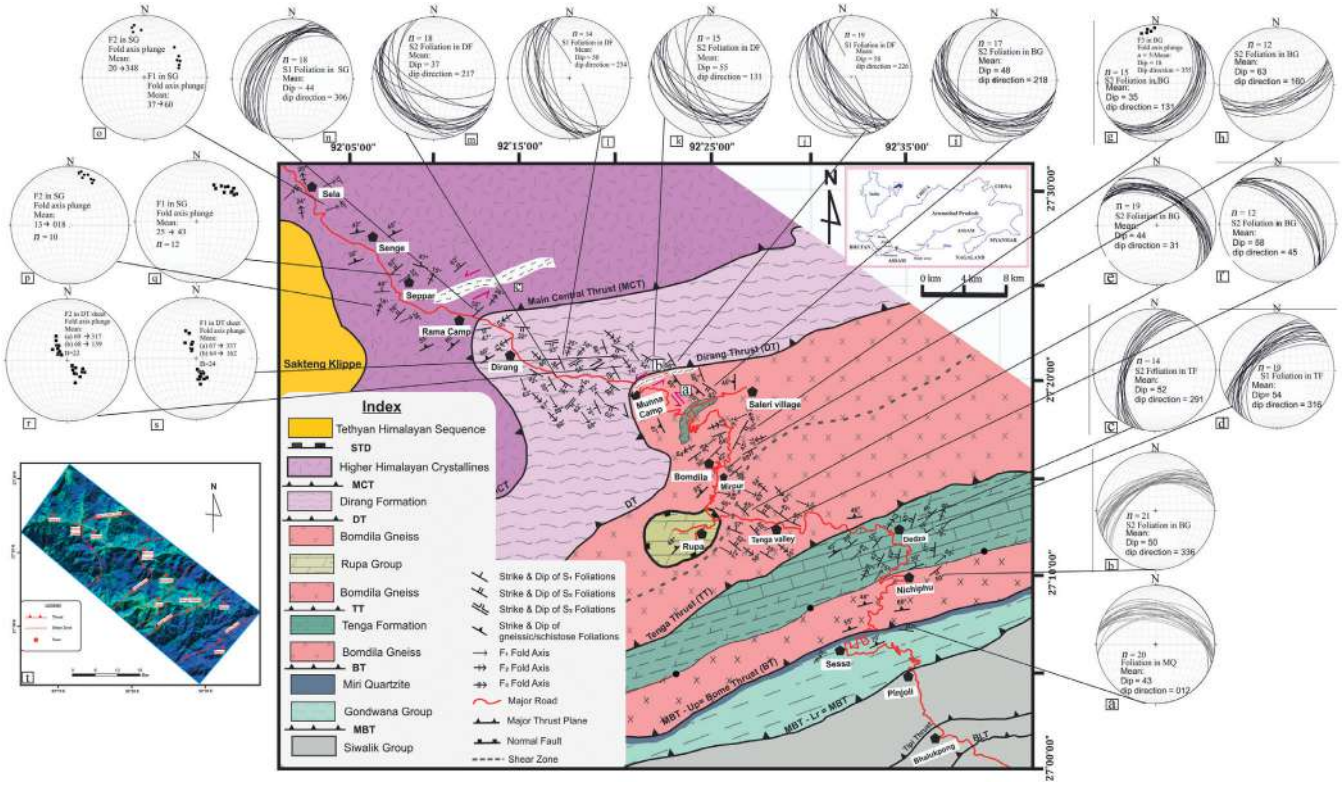

FIGURE 3 Field structural data from Dedza–Dirang–Sela area plotted on the map (modified from DeCelles et al., 2016; Yin et al., 2010a). The modification of the map is based the field traverse of the authors in the area. Equal area and lower hemisphere plots of the bedding, foliation, and fold axis of different phase of deformation are data from the area: (a) Foliations in Miri quartzite in the north of Sessa; the foliations dip towards NE. (b) S2 foliation in Bomdila gneiss (BG) in the south of Nichiphu shows dominant dip towards NNW. (c,d) S1 and S2 foliations in the quartz mica schists of the Tenga Formation around Dedza dipping to WNW and NW directions at moderate angles (~53°). (e,f) S2 foliation in BG in two places: At Rupa junction and at Birpur show dominant dip towards NE direction. (g,h) S2 foliation in BG shows change of dip direction from SE to southerly at 20 km north of Bomdila. F3 folds recorded in BG dips at low angle to northerly direction. (i) The BG shows strike of the dominant S2 foliation along NW-SE dipping moderately (48°) towards SW direction. (j) S1 foliation in quartz mica schists of Dirang Formation (DF) shows NW-SE orientation dipping to SW direction. (k) S2 foliation in DF shows WNW orientation dipping to SW direction. S2 orientations are however affected by the subsequent deformation episodes. (l–n) S1 and S2 foliations of the DF show dominant dip to SW direction. (o–q) Shows plunge of the F1 and F2 fold axis to NE and NW directions respectively. (r,s) Depicts plunge of the F1 and F2 fold axis of the DF to NW and SE directions at steep angles (~68°). (t) The DEM of the study area where major thrusts are drawn

4 | RESULTS

4.1 | Deformation pattern in the basal LHC

We documented mesoscopic structures of the LHC and the HHC for ~146 km along a NW–SE-traverse from Dedza to Sela. The planar and the linear fabrics in the rocks signifying pervasive ductile deformation were noted in the scales of cm up to tens of meters. The present study documents the structural data for different phases of deformation in the basal unit of the LHC from Dedza to Tenga (Figure 3).

Three phases of deformation (D1–D3) were documented in the schistose rocks of the basal LHC. D1 is imprinted with tight isoclinal recline type F1 folds with attenuated and detached limbs in the metapelites of the Tenga Formation. F1 fold hinge line plunges at 51° to NE at 10 km NNE of Nichiphu (i.e., 40% of the F1 fold hinges plunges to NNE), 78° to SW direction at Dedza (i.e., 35% of the F1 fold hinges plunge to SW) and 72° to ENE at 15 km NNW of Dedza (i.e., 25% of the F1 fold hinges plunge to NNW). The axial plane schistosity S1 of the F1 folds dip dominantly to NW direction (Figure 4a). The F1 and F2 fold axes plunge are also represented through a line diagram (Figure 4a). The curvature of the S1 axial planar cleavage of the F1 folds is due to the effect of the subsequent deformation. The F1 folds are refolded to open (interlimb angle ~90°) asymmetric F2 folds where the axial plane schistosity S2 trends NNE (i.e., 65% of the S2 trends NNE) or NE (i.e., 35% of the S2 trends NE) and dips steeply to WNW (i.e., 80% of the S2) and NW (i.e., 20% of the S2) directions. The F2 hinge lines plunge to NE or NNE or SSW directions. The F1 and the F2 folds display coaxial refolding and curved S2 schistosity (Figure 4a). The D3 deformation is manifested by the open F3 folds that plunge to NW direction at a moderate angle (30–35°). The competency contrasts in the case of the multi-layered open F3 folds are observed as the phyllite layers show kink folds in comparison to the open folded quartzite layers (Figure 4b). S2 schistosity in BG defines the syn-Himalayan intense intracontinental ductile shear fabric discussed in the following section.

4.1.1 | Top-to-SE shear in BG

The ductile shear fabrics in the Bomdila Gneisses (BG) include S-C structures, asymmetric porphyroblasts, and asymmetric folds. These pervasively developed fabrics were studied for shear sense. Mesoscopic F1 fold and associated S1 axial planar foliation are not observed in the BG. Himalayan deformation (D2 episode) is

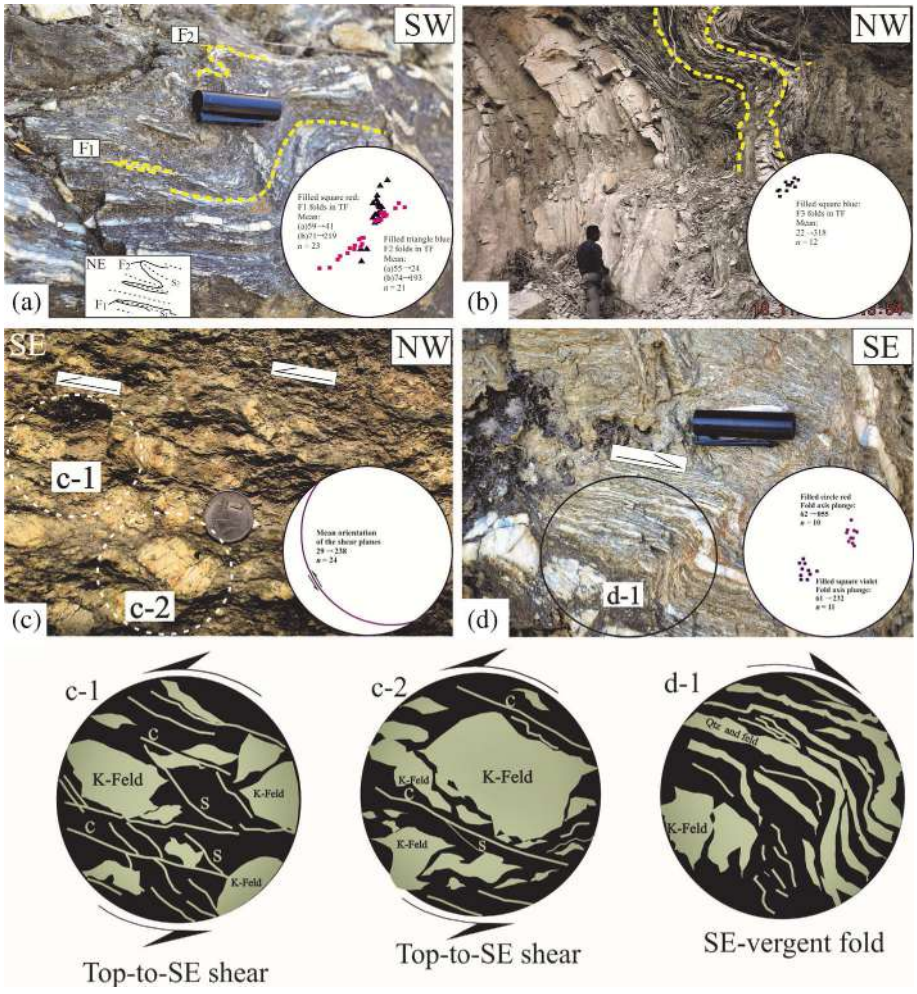

FIGURE 4 (a) F1 and F2 axes in the quartz mica schists of Tenga Formation. The axes plunge at moderate to high angle (55–74°) to NE and SW direction. F1 and F2 folds show coaxial refolding. Inset line drawings: F1and F2 axial traces and fold axes. (b) F3 open folds in the quartzite inter-layered with phyllite at Tenga. The fold axis plunge ~22° towards NW. (c) Mylonitic Bomdila gneisses at 18 km from Bomdila towards Dirang. The mean shear plane trends NW–SE. The asymmetric K-feldspar porphyroclasts, S-C atructures and top-to-SE shear is depicted through c-1 and c-2. (d) SE vergent F2 folds in BG at Birpur. The fold axis plunge to NE and SW at ~62°. The folded mylonitc foliation verging SE is depicted through d-1

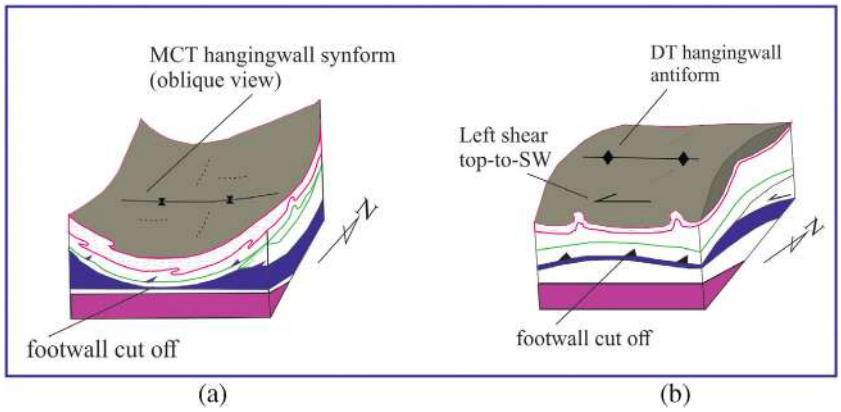

FIGURE 5 (a) Synformal MCT plane (Bhattacharyya and Nandy, 2008) and cuspate thrust trace (concave outward) in the longitudinal section (modified from Ray, 1995, Figure 11). The early F1 folds verge to NE and are parallel to the thrust plane. The F2 hinge trend NW-SE and parallels the cuspate thrust trace. (b) The antiformal DT plane and the longitudinal section of the cuspate thrust trace which parallels the mesoscopic F2 folds in the DT sheet. The thrust trace may also depict syn-thrust shear in the DT zone where top-to-SW sense (to the left) is depicted

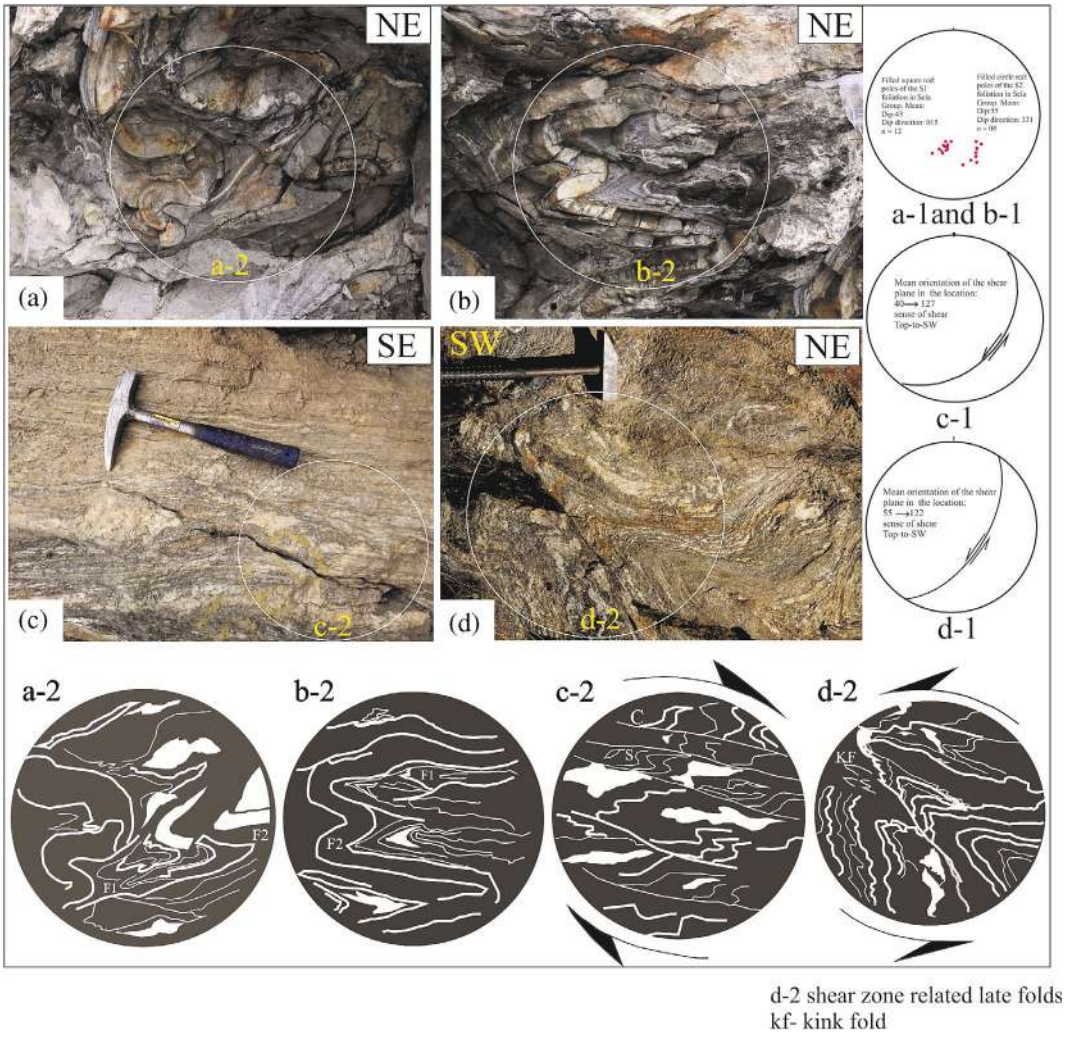

FIGURE 6 (a,b) F1 and F2 folds in the psammitic gneisses of the Sela Group (46 km from Seppar). The F1 and F2 folds are coaxially refolded. The hinges of the tight F1 folds are thick and fold axis plunge to ENE or WSW direction. The F2 folds depict class-2 geometry of Ramsay 1967, and the fold axis plunge at low angle to the NE or SW directions. In a-2 and b-2, the line diagrams further magnify the fold geometry. (c,d) Ductile shear in mylonitic meta-psammites at sapper. In (c), the S-C structure depicts top-to-SW sense of shear; the S and C make acute angle (~15°) relation. (d) The shear related folds gradually becomes sharp hinge chevron type towards left and records the end phase of the ductile deformation with shorter limb got dissected—see left part of the photograph. The line diagram (d-2) further illustrates the geometry. KF, Potash feldspar

synchronous with the exhumation and ductile shearing with composite S-C planar fabric. S2 schistosity represents the regional schistosity plane and may be considered as parallel to the intense intracontinental ductile shear of the D2 episode along which all earlier structures are transposed (Jain, Singh, & Manickavasagam, 2002). The pervasive regional ductile shear in BG may be parallel to the S2 foliation. Two dominant trends of the S2 foliations are noted in BG (ENE and NE), the dominant trend being the ENE. The foliations dip at moderate angles (~50°) to WNW, NW, or NE directions (Figure 3b,e–i). This indicates a shortening from the NNE direction. The C-plane dips ~60° to ENE and trends NW-SE in the north of Bomdila. Near the contact with DT, the S2 within the BG trends NW and dips ~48° towards SW. The S and the C planes make acute angle relation and the angle decreases considerably (~40–10°) near the contact of BG and the DT in the north. A top-to-SE shear sense is recorded from the BG (Figure 4c).

Barring the symmetric clasts (Mukherjee, 2017), sigmoid porphyroblasts analogous to sigma-structures have their major axis tilted towards the shear direction (Figure 4c). The spacing of the C-planes varies ~2–12 cm. The intensity of shear in BG can be noted from the spacing of the C-planes. The spacing is reduced considerably in the highly sheared portions. In the south, near the contact with the Tenga Thrust, asymmetric folds (Mukherjee, Punekar, Mahadani, & Mukherjee, 2015) in the mylontic foliation (S-C composite) depict top-to-south shear in the BG (Figure 4d). The sigmoid porphyroclasts are composed of feldspars and the sheared matrix is dominated by quartz, feldspar, and mica. Sigmoid feldspar porphyroclasts, asymmetric lenses of quartz, and feldspar and quartz vein showing sigma-like structures indicate the shear sense (Figure 4c,d).

Thus, the mesoscale structures in the mylonitic BG reveal a strong imprint of Himalayan deformation. The earlier fabric of the Proterozoic Lesser Himalayan basement is completely transposed/obliterated (Sarma et al., 2014).

4.2 | Deformation across MCT and DT zones

Here we primarily discuss the deformation pattern in the rocks of the DF (the upper unit of LHC), the Dirang Thrust (DT) zone, rocks in the MCT hangingwall, and the MCT zone specifically.

Internal deformation of thrust sheets is generally characterized intriguingly by folds of different orientations and the associated development of fabrics (Rattey & Sanderson, 1982). There may be differential displacements between adjacent tip points of large thrusts associated with folding and eventually these faults are segmented and linked through smaller fault segments (Ellis & Dunlap, 1988). Further, the trace of major crustal-scale thrusts may exhibit cuspate and lobate structures of the thrust plane in lateral sections. These types of

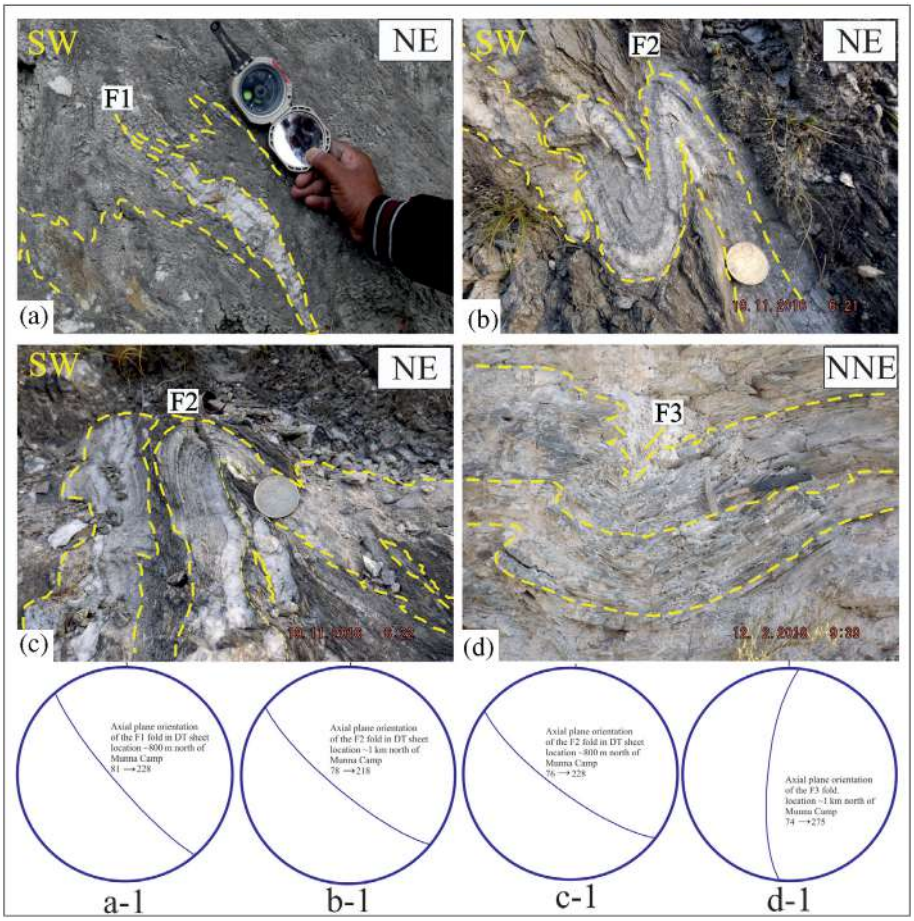

FIGURE 7 Deformation in Dirang Thrust sheet. (a) Tight isoclinal F1 folds in DT sheet. The fold axis plunge (~69°) to NW or SE direction. a-1 shows axial plane orientation of the F1 folds. (b,c) Close asymmetric F2 folds in DT sheet ~1 km north of Munna camp. Fold axis plunge ~70° to NW or SE direction. b-1 and c-1 shows orientation of the axial plane in F2 folds in DT sheet. Both F1 and F2 folds verge steeply (~80°) to SW direction. (d) The open, nearly upright F3 folds in DT sheet (~1 km north of Munna camp) show NNE–SSW trending axial plane (depicted in d-1) orientation and the fold axis plunge at low angle to northerly direction

cuspate and lobate structures are observed in Shumar thrust in eastern Himalaya and viewed along lateral and transverse sections (Ray, 1995). The Shumar thrust displays a scoop-shaped structure (listric fault with curvi-planar or concave upward fault surface. The fault surface becomes horizontal with increasing depth) and is imprinted occasionally with ridges parallel to the direction of thrust movement. Significantly, the NE-dipping axial surfaces of the earliest folds in the hangingwall progressively reorient temporally parallel to the thrust plane (Ray, 1995).

Published maps and our field data from the area indicate that the MCT and DT in the western Arunachal display a recess or 'concave to the foreland' thrust trace in a synformal (MCT) and antiformal (DT) hangingwall over a footwall ramp (Bhattacharyya & Nandy, 2007; DeCelles et al., 2016; Yin et al., 2010b). The HHC in the hangingwall of the MCT is folded into a broad synform (Bhttacharyya & Nandy, 2008; DeCelles et al., 2016). We have observed that in the hangingwall of MCT, north of Sela, early folds verge towards NE (Figure 5a). However, in the MCT ductile shear zone at Seppar, the sense of shear is top-to-SW and this is in conformity with the Dirang Thrust zone at Munna Camp, where the outcrop scale kinematic indicators depict same top-to-SW shear (Figure 5b).

4.2.1 | Thrust parallel shear at the MCT zone

Quartzites and calc-silicates in the hangingwall of the MCT at Sela are tightly/isoclinally folded with hinge lines plunging ~62° towards ENE (76°; Figure 6a,b). The axial planar schistosity of F1 folds dips ~43° towards NNW (015°) direction. The F1 folds are refolded by open F2 folds observed in psammitic schists and gneisses. The axial plane schistosity of the F2 folds dips ~48° towards NW or SE, whereas the F2's hinge line plunges at low-angle (~18–24°) towards NE. The F1

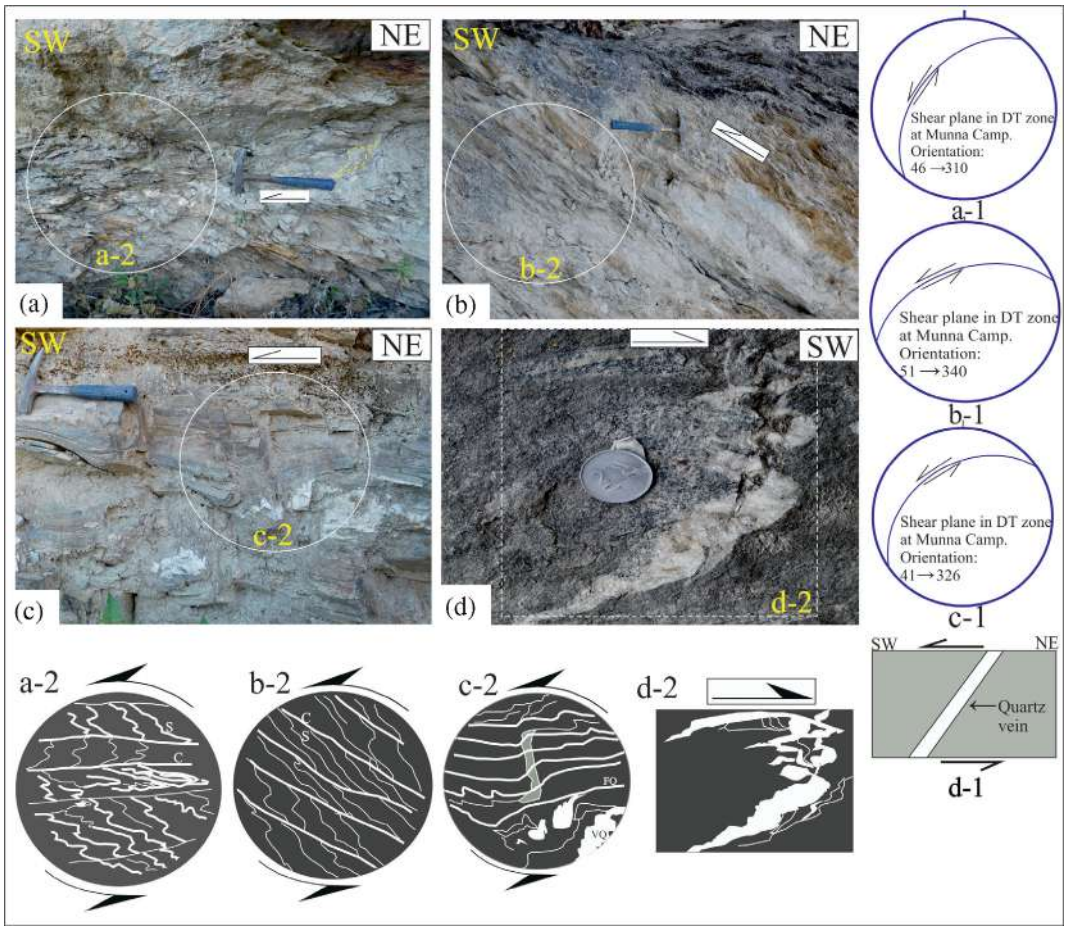

FIGURE 8 Dirang thrust zone at Munna camp. (a,b) S-C structure in quartz mica schists. The sense of shear is top-to-SW (to the left). The S and C are making acute angles (~30°). The shear plane orientations are ~NE–SW and dips ~50° towards NW direction (a-1 and b-1). a-2 and b-2 depicts S-C structure through line diagrams. (c) The inter-layered quartzites and phyllites display boudin like structure. The shear plane orientation is shown in c-1. The foliated quartzite (FQ) and vein quartz (VQ) are depicted in c-2. (d) The folded vein underwent top-to-SW shear. The initial orientation of the quartz vein is NE–SW (d-1) due to top-to-left (SW) shear, the vein is folded and the folds verge towards both NE and SW directions. The vein may be mimicking F1/F2 folds initially and suffered ductile shearing during late D2 phase of deformation. Line diagram (d-2) further depicts the sinistral and dextral vergence of the folds in the quartz vein

and the F2 fold hinges are sub-parallel and together they are refolded almost coaxially (Srivastava et al., 2011).

About 10 km north of the Rama camp (27°24.7′47″N: 92°07.97′9″E), the ductile deformation in mylonitic meta-psammites is documented at Sapper (27°24.7'47″N:92°07.9'79″E). The mylonitic fabrics display asymmetric lenses and shear-related folds (Figure 6c,d). These folds verge dominantly towards SW. 80% of the total number of folds show this vergence. The tight isoclinal folds in Figure 6d are refolded into open asymmetric folds and closing in opposite directions. The tight isoclinal (chevron) fold is dissected in the shorter limb on the left (Figure 6d).

4.2.2 | Deformation in the rocks of DF

The LHC of the DF, in the hangingwall of DT, is folded thrice. The outcrop-scale early first-generation tight folds are mapped at 800 m NNW from Munna Camp at ~1 km from the north-western outcrop of the BG (27°19′40.1″N:92°21′59.8″E). The axes of the F1 folds plunge ~69° towards NW or SE. Therefore, the F1 axis trends transverse to the orogenic trend. These F1 folds verge towards SW or SSW and are thicker in the hinges (Figure 7b). The short limbs of the asymmetric folds are attenuated, sheared-off, and displaced. Initial horizontal orientation of the F1 folds is considered parallel or sub-parallel to the thrust plane (Figure 5a,b). F1 folds reoriented during the folding of the thrust plane (Figure 5b). Therefore, from the present disposition of the F1 folds, these are interpreted to be Himalayan. Here, we interpret that the reorientation of the F1 folds is due to folding and synchronous ductile left shear along the thrust zone, which have also affected the early folds in the immediate hangingwall of the thrust zone (Figure 5b). The F1 folds are superposed by close F2 folds in quartzite documented only at ~1 km north of the Dirang Thrust Zone at Munna Camp (Figure 7b). These close folds are reclined type and axis plunge around 64–67° to NW, WNW, or SE, or ESE directions (Figure 7c). The axial plane schistosity of F2 folds dip steeply to NE direction. The near parallelism of the F1 and F2 hinge lines are noted (Figure 7a–c). The open asymmetric folds at ~6 km NW from Munna Camp display a progressive decrease in the deformation in response to a ~N–S compression. The asymmetries of the open folds in inter-layered quartzite and phyllite is towards NNE and the hinge line of the folds plunges at a low angle (20–30°) to NNE or northerly direction (Figure 7d).

4.2.3 | Thrust parallel shear at DT zone

At Munna camp, ~ 60 m thick mylonitic zone in metapelites differentiates it from the Bomdila gneisses in the south. The mylonitic inter-layered metapelites and metapsamites display a top-to-SW sense of shear (Figure 8). The lithologic layers (S_0) are deflected by shear

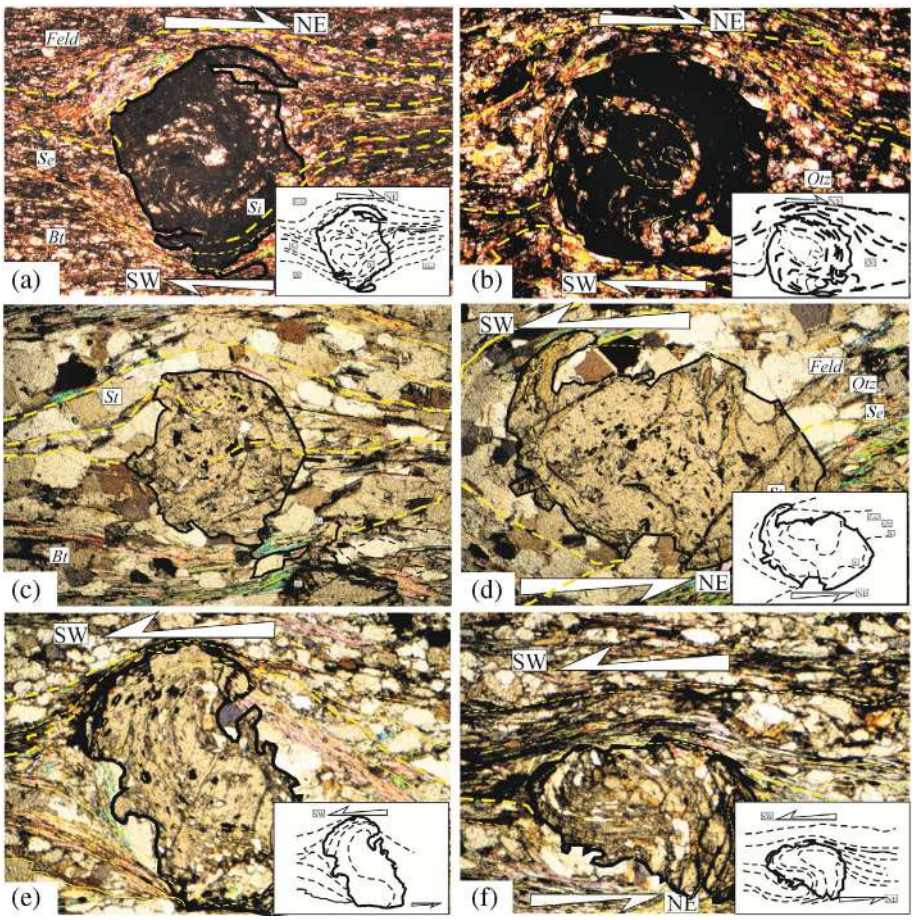

FIGURE 9 Garnet inclusion trail geometry in DT sheet: Spiral shaped inclusion trails in the core of the garnet porphyroblasts. (a,b) Top-to-NE rotation of the inclusion trails in the higher structural level (1 km north of Munna camp) the inclusion trails are composed of quartz, muscovite, biotite, epidote and plagioclase and the garnets are snowball shaped. (c) This garnet grain is not used for shear sense determination. (d–f) Top-to-SW rotation of the inclusion trails in the lower structural level in the immediate north (~500 m) of DT zone of Munna camp. All photographs in ×4 magnification. (a,b) In CPL and (c–f) in PPL. Bt, biotite; Feld, K-feldspar; Mus, muscovite; Qtz, quartz; Se, external foliation; Si, internal foliation; St, staurolite (detail in Section 4.2.4)

TABLE 2 (a) Geometrical measurements of the garnet porphyroblast from higher structural level of DF (total garnet analysed = 28. Sense of rotation: Top-to-NE). (b) Variation in the values of α, β and R

(a)

Sl no	α (in degree)	β (in degree)	R (unitless)
1	205	92	1.37
2	180	90	1
3	196	100	1.46
4	182	92	1.12
5	204	95	1.28
6	200	90	1.2
7	190	98	1.1
8	188	102	1.05
9	202	90	1.36
10	182	91	1.1
11	194	104	1.48
12	180	93	1.14
13	206	96	1.3
14	198	92	1.26
15	186	104	1.08
16	184	94	1.12
17	188	104	1.04
18	201	91	1.34
19	192	96	1.08
20	191	95	1.07
21	203	91	1.31
22	199	93	1.1
23	200	92	1.11
24	187	101	1.02
25	185	93	1.09
26	189	96	1.09
27	138	46	1.45
28	226	96	1.26

(b)

α variation		β variation		R variation	
Number of observation	Range (in degree)	Number of observation	Range (in degree)	Number of observation	Range (in degree)
0	0–30	0	0–30	19	1.0–1.2
0	30–60	1	30–60	7	1.2–1.4
0	60–90	3	60–90	2	1.4–1.6
0	90–120	24	90–120	0	1.6–1.8
1	120–150	0	120–150	0	1.8–2.0
2	150–180	0	150–180	0	2.0–2.2
24	180–210	0	180–210	0	2.2–2.4
1	210–240	0	210–240	0	2.4–2.6

Note: See text for details in Section 4.2.4.

TABLE 3 (a) Geometrical measurements of the garnet porphyroblast from lower structural level of DF (total garnet analysed = 26. Sense of rotation: top-to-SW). (b) Variation in the values of α, β and R

(a)

Sl no	α (in degree)	β (in degree)	R (unitless)
1	132	55	2
2	130	42	2.2
3	176	24	1.75
4	136	48	2.1
5	140	40	2
6	180	26	1.8
7	135	53	2.32
8	132	45	1.98
9	131	52	2.1
10	142	54	1.96
11	138	51	2.2
12	172	26	1.78
13	144	42	2.2
14	174	26	1.76
15	178	22	1.72
16	170	28	1.8
17	146	44	1.98
18	168	32	1.78
19	167	33	1.76
20	166	34	1.76
21	178	21	1.71
22	180	25	1.79
23	173	27	1.77
24	110	40	2.35
25	190	24	1.78
26	132	54	1.97

(b)

α variation		β variation		R variation	
Number	Range	Number	Range	Number	Range
0	0–30	0	0–10	0	1.1–1.2
0	30–60	1	10–20	0	1.2–1.4
0	60–90	10	20–30	0	1.4–1.6
1	90–120	5	30–40	1	1.6–1.8
12	120–150	5	40–50	12	1.8–2.0
12	150–180	6	50–60	12	2.0–2.2
1	180–210	0	60–70	1	2.2–2.4
0	210–240	0	70–80	0	2.4–2.6

Note: See text for details in Section 4.2.4.

foliation (C) producing S-C structures. The angle between S and C planes falls from 35 to 28° in the metapelites (Figure 8a). The psammites/pelites display top-to-SW shear (Figure 8b). The

asymmetric sigmoids in psammites also show the same shear sense. Interlayered phyllite in psammites displays boudins at 200 m to the NW of the location of Figure 8a,b. The asymmetry in boudins with top-to-SW shear is noted (Figure 8c). In quartzitic psammites, quartz veins are folded with short wavelengths. The initial orientation of the vein is as shown in the inset (d-1). Figure 8d is an example of a vein folded due to shear under NE–SW compression.

4.2.4 | Garnet inclusion trail geometry in the rocks of DF

In a collisional orogen, the regional tectonic strain may often be parallel to the principal directions of the finite strain in the outcrop-scale or regional orientation of the folds or major shear zones (Ilg & Karlstrom, 2000). Thus, the inclusion of trail geometry within porphyroblasts is a good proxy for studying the history of rock's deformation, through the interpretation of the fabrics that define porphyroblast-matrix interrelationships (e.g., Aerden, 1998; Bell, Rubenach, & Fleming, 1986). The geometry of the garnet prophyroblast inclusion trails in the rocks of DF is studied to understand the phenomena of whether the rigid body rotation is in conformity with the sense of the shear in the ductile Dirang thrust or shear zone.

The pelitic schists of the DF dominantly contain garnet, biotite, muscovite, and quartz. Garnet in the metapelites is invariably recorded from the thrust contact of the DF with the BG at Munna Camp to the higher structural level up to Rama Camp. At the higher level, kyanite is recorded along with garnet and progressive increase

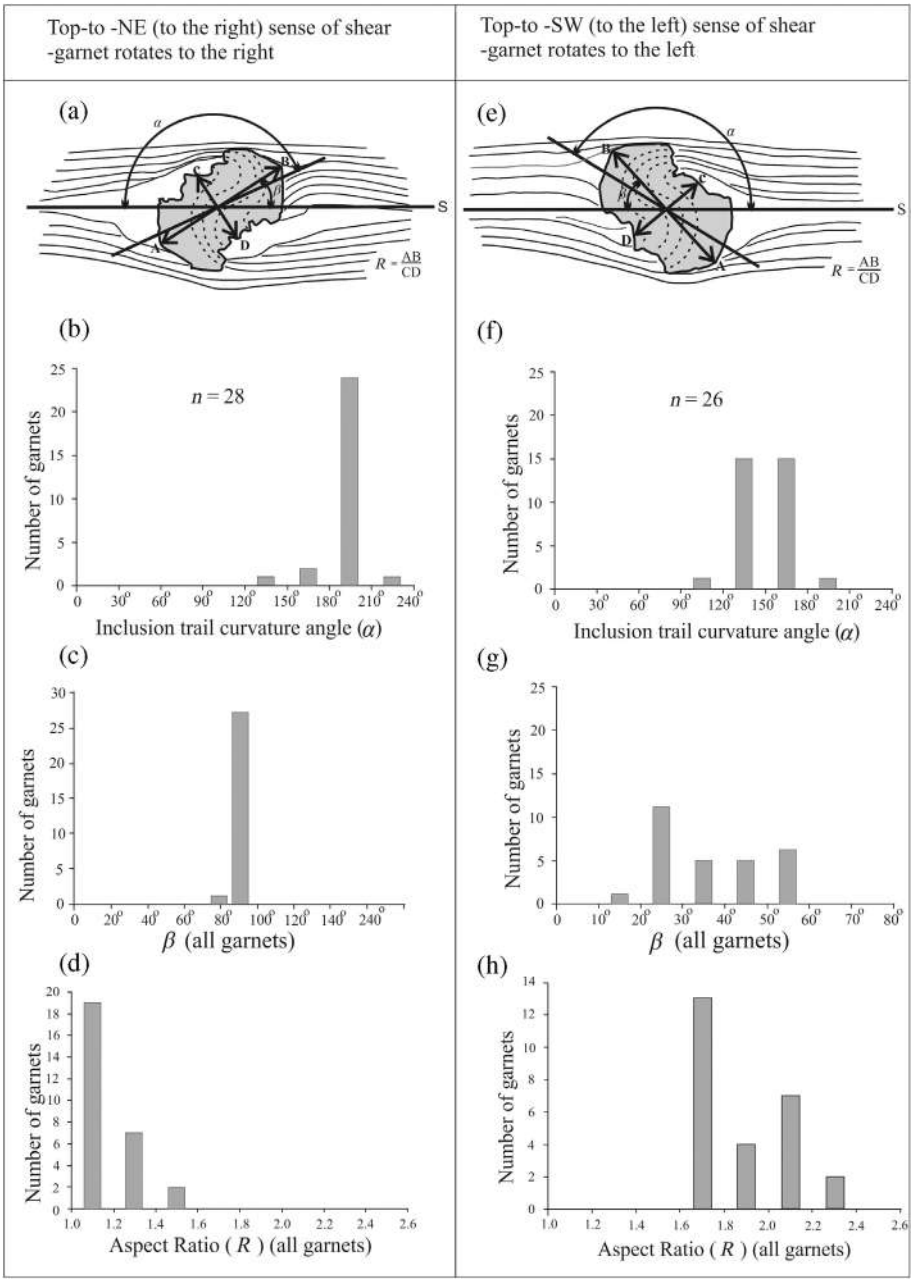

FIGURE 10 The measured values of α, β and R in the higher to lower structural horizon of the DT sheet: (a) depicts the measurement of inclusion trail curvature angle (α), the β angle and aspect ratio R of the garnet porphyroblasts for the upper structural horizon. (b–d) Histogram for 28 garnets in the upper structural level for α, β and R variation among the porphyroblasts. (e) Measurement of α, β, and R values for garnets of lower structural horizon. (f–h) Indicates the α, β, and R variation in 26 garnets through histograms

in the size of the garnet is noted. The oriented thin-sections from the DT sheet indicate that the garnet porphyroblasts are snowball-shaped with spiral inclusion trails composed of quartz, muscovite, biotite, epidote, and plagioclase. The S1 foliations in the rocks are defined by muscovite and biotite and these foliations are overprinted by pervasive S2 foliations (Figure 9). At the higher structural level, chlorite and ilmenite are also recorded in the inclusion trails along with muscovite, biotite, and epidote (Goswami et al., 2009). Therefore, rocks in the hangingwall of DT offers an ideal setting for correlating deformation history and microstructures.

The inclusion trails in garnet porphyroblasts are spiral-shaped in the core whereas the rims are inclusion-free. The porphyroblasts are wrapped by S2 foliations and quartz grains in the pressure shadow zones are noted (Figure 9). This suggests syntectonic growth of the porphyroblasts during D1 deformation and the porphyroblasts show top-to-NE shear in the higher structural level in the north DT (~5 km) zone. In a few cases, garnet porphyroblasts (Figure 9c) are not considered for shear sense since those have non-conclusive patterns of inclusions. The subsequent anticlockwise rotation of the porphyroblasts is interpreted to be pre-tectonic to the development of pervasive S2 foliations (Bhattacharyya and Nandy, 2007) and this is recorded in the lower structural level (~200 m north from DT zone). The rotation of the inclusion trail (Si) in the garnets in the metapelites in these two structural horizons in the hangingwall of Dirang Thrust is illustrated in Figure 9a–e.

Geometrical measurements (Tables 2 and 3) of the porphyroblasts in the pelitic schists in the DT sheet in the lower (Table 2) and higher (Table 3) structural levels are carried out as per Trouw, Tavares, and Robyr (2008). The inclusion trail curvature angle (α) is the angle between the tangent of the inclusion trail in the porphyroblast centre and average matrix foliation (S2); aspect ratio (R) is the ratio between longest and shortest dimension (AB and CD in Figure 10) of the

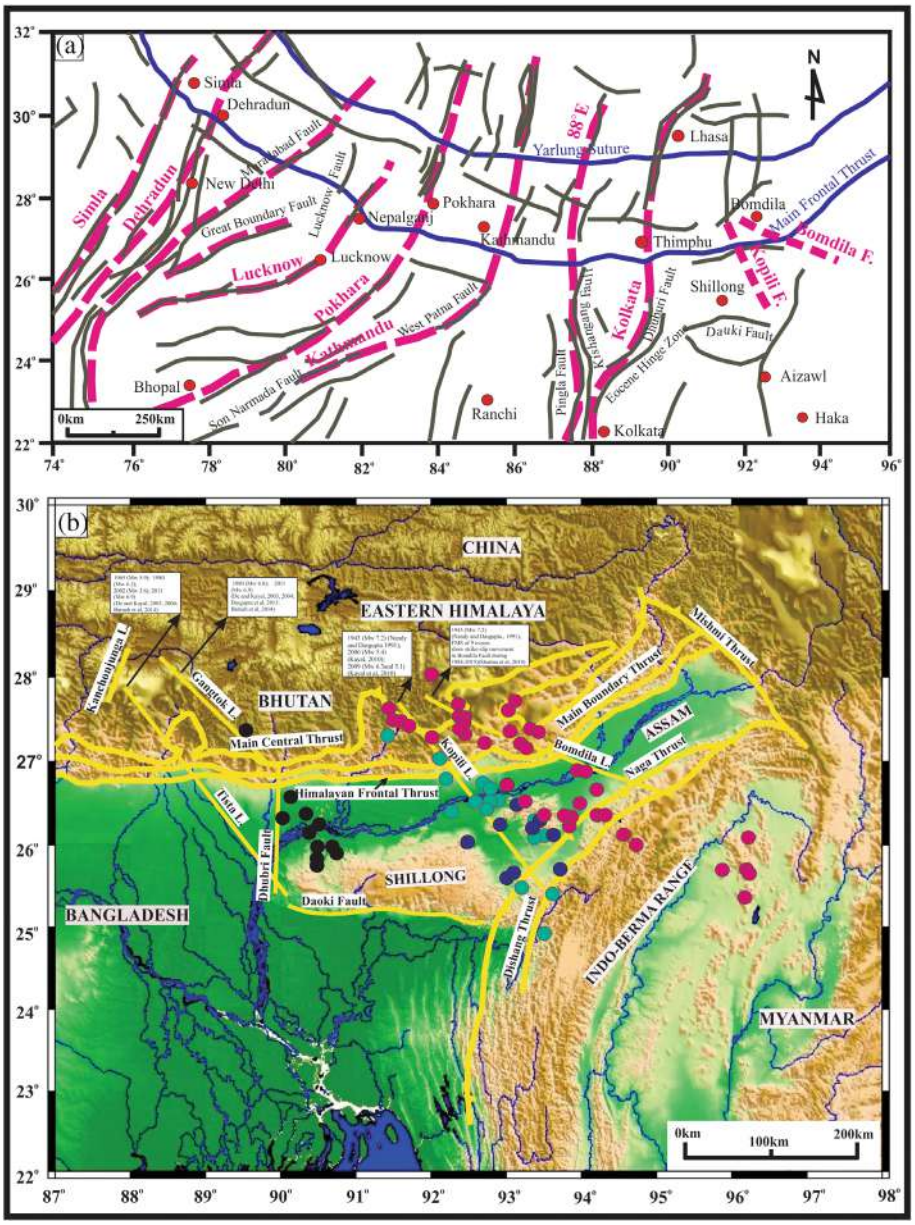

FIGURE 11 (a) The location of the major Indian basement ridges, major graben systems and traces of the major lineaments in the western and central Himalaya are shown (modified from Figure 8, Godin & Harris, 2014). The major orogen transverse basement lineaments are shown as red dashed lines which connect the underplated Indian faults with upper crustal graben faults on the overlying crust in the north of the MFT. (b) Map of eastern Himalaya showing major cross-stirke faults (Kanchenjunga, Tista, Gangtok, Dhubri, Kopili, and Bomdila). Seismicity mainly associated with Kopili and Bomdila faults, plotted from Sharma et al. (2018) for 188 FMS and shown through green, blue, and red circles. The magnitude and year of major earthquakes showing strike-slip focal mechanism presented for Tista, Gangtok, Kopili, and Bomdila faults along with references

crystal and 'β' is the angle between longest dimension of the crystal and average matrix foliation (S2) (Figure 10a,e).

The measured values of α, β, and R for 28 garnets in the higher structural level (Table 2) in the DT sheet and 26 garnets in the lower structural level (DT zone) (Table 3) are shown in Figure 10a–h. In the higher structural level, the inclusion trail curvature angle of garnet porphyroblasts (α) clusters around 200°, and β values do so at ~90°. The values of aspect ratio (R) are ~1 (1.0–1.48) (circular grains 52%). This indicates that the garnet porphyroblasts developed almost up to the spherical shape. In the lower structural level near the DT zone, α values range between 110 to 190° and β values cluster within the 0–90°. The aspect ratio (R) values range from 1.71 and 2.35. The R values of these garnets indicate that these are less spherical and poorly developed. Further, the β value clustering ~90° indicates a long axis and the growth of the porphyroblasts is orthogonal to average matrix foliation and R-value approaches to 1-which is observed in the upper structural level.

The inclusion trails in the garnet grains from quartz–mica schists at Dirang shows top-to-NE shear and this reverses to top-to-SW in the sheared metapelites at Munna camp. The top-to-SW shear senses are recorded both from the Seppar and Munna camps in the MCT and DT zones (Figure 2).

MCT zone defines the high-strain zones of ductile deformation, along which the Tertiary metamorphic rocks of the HHC place over the low-grade LHC rocks. Further, the MCT zone marks the base of the inverted metamorphic sequence (Martin, 2016). DT zone signifies the ductile deformation at the base of the Dirang Formation. Along DT zone, the LHC of the Dirang Formation places over the Bomdila Gneisses. The Bomdila Gneisses represent the lower unit of the LHC (Table 1).

5 | SEISMOTECTONICS

Along-strike variation of seismicity in the western and central Himalaya due to the buried Indian basement ridges and major lineaments (discussed in Section 1) are shown in Figure 11a. In the eastern Himalaya, the Bomdila Fault is 400 km long and extends in a WNW direction from the belt of schuppen to the MCT zone in the HHC, Arunachal Pradesh. In the Bomdila Fault zone, large concentrations of the earthquake takes place in the depth of 50 ± 2 km and the fault is very active in its northern part (Sharma et al., 2018). The Bomdila Fault zone is marked by the ductile fabrics in the mylonitic Bomdila Gneisses with top-to-SSE shear. The focal mechanism solution of the earthquake events characterize the Bomdila Fault to be strike-slip. The inference of its strike-slip nature is further supplemented by gravity, magnetic, and neotectonic evidences (Sharma et al., 2018), Stress inversion results indicate a near N-S compressional stress (σ_1) and an E-W extensional stress (σ_3) for the formation of the Kopili-Bomdila fault system. The magnitude of σ_1 is dominant within ~0–30 km depth (Baruah & Kayal, 2013). Figure 2c presents the direction of the minimum compression axis (Verma, 1985).

TABLE 4 Generalized stratigraphic succession in the north bank of Brahmaputra River (after Bharali et al., 1999)

Age	Group	Formation	Description	Thickness in m
Recent and Pleistocene		Alluvial and high-level terraces	Unconsolidated to semi-consolidated sandstone with minor silt stone bands	800–1,200
Pliocene	Dihing	Dhekiajuli Beds	Sandstone with siltstone beds	800–1,000
Unconformity				
Mio-Pliocene	Dupitila	Namsang Beds	Sandstone with interbeds of clay and occasional carbonaceous matter	400–1,000
Unconformity				
Mio-Pliocene	Tipam	Girujan Clay	Mottled clay with sandstone	0–100 (absent in Bihpuria Well-A)
		Tipam Sandstone	Sandstone with interbeds of silty clay and occasional presence of coal in the lower part	400–1,800
Unconformity				
Oligocene	Barail	Barail argillaceous and arenaceous	Alternation of argillaceous shale and coal bands with subordinate sandstone with minor shale bands	0–4 but absent in Bihpuria Well-A
Unconformity				
Eocene/Upper Palaeocene	Jaintia	Kopili	Shale, Siltstone, claystone, alternations of carbonaceous shale and calcareous sandstone	200–280
		Sylhet Limestone	Fossiliferous limestone, streaks with shale and sandstone	100–300
Precambrian	Basement complex	Basement	Granite/granitic gneisses	

The present study attempts to link the surface deformation features in the MCT zone and the deformation in the Indian basement with the seismicity in the region. It is significant to note that earthquakes with >40 km focal depth are associated with underthrusting of the deformed Indian basement in the eastern Himalaya (Paul, Mitra, Bhattacharya, & Suresh, 2017; Sharma et al., 2018).

Field signatures of the MCT zone (high-grade rocks, orthogneisses with leucogranite sills filling cracks and fissures) in the Himalaya indicate ductile deformation exhumed rocks from below the brittle–ductile transition zone (at depths of 15–18 km) (Searle, Avouac, Elliot, & Dyck, 2017). There are records of great earthquakes in the Himalaya without any significant signatures of surface slip through brittle thrusting south to MCT (Searle et al., 2017 and references therein).

Figure 11b presents the focal mechanism solution of earthquakes along the Kopili and the Bomdila faults (modified from Sharma et al., 2018). Out of the 40 focal solutions along the Kopili Fault, 23 show strike-slip movement (green circles). Out of the 12 events associated with the Bomdila Fault, nine- show strike-slip faulting (red circles) during 1984–2015 (Sharma et al., 2018). The NW part of the Bomdila Fault is more seismic than its SE portion.

Further, the earthquake database (ISC and USGS) of 1285 seismic events for the last 30 years (1990–2020) with Mw 4.0–6.6 with 4–200 km focal depth was used to prepare the epicentral location map (Figure S1).

In the eastern Himalaya, the orogen perpendicular structures are projections from transverse faults in the underthrust Indian basement. These faults (Kanchenjunga, Tista, Gangtok, Goalpara, Kopili, and Bomdila) create active seismic segments (Dasgupta et al., 2013; De & Kayal, 2004; Kayal et al., 2010; Sharma et al., 2018). The stress build-up in the region is also due to the movement along the cross-strike Dudhnai Fault (Hossain, Khan, Abdullah, & Mukherjee, 2021). The NNE and NNW-trending basement faults like the Monghyr-Saharsa Fault or the Malda-Kishanganj Fault continue beneath the Himalaya northward and are manifested as NNE-trending Kanchenjunga lineament or the NNW-trending Tista lineament in the Sikkim Himalaya (Dasgupta et al., 2013). Strike-slip motion along the Tista Lineament caused two major earthquakes in 2007 and 2011 with focal depths of ~42 and ~51 km, respectively (Dasgupta et al., 2013). Baruah and Kayal (2013) found that out of 516 focal mechanism solutions for earthquakes in the eastern Himalaya, from 1974 to 2011, 234 show strike–slip focal mechanism. The depth range for these earthquakes is 5–150 km and the magnitude range is 2.5–8.6.

The 2011 Sikkim earthquake (Mw 6.9; focal depth 50 km) is associated with a vertical fault with dextral slip and the displacement is either along Tista or along Kanchenjunga Fault (Baruah et al., 2016;

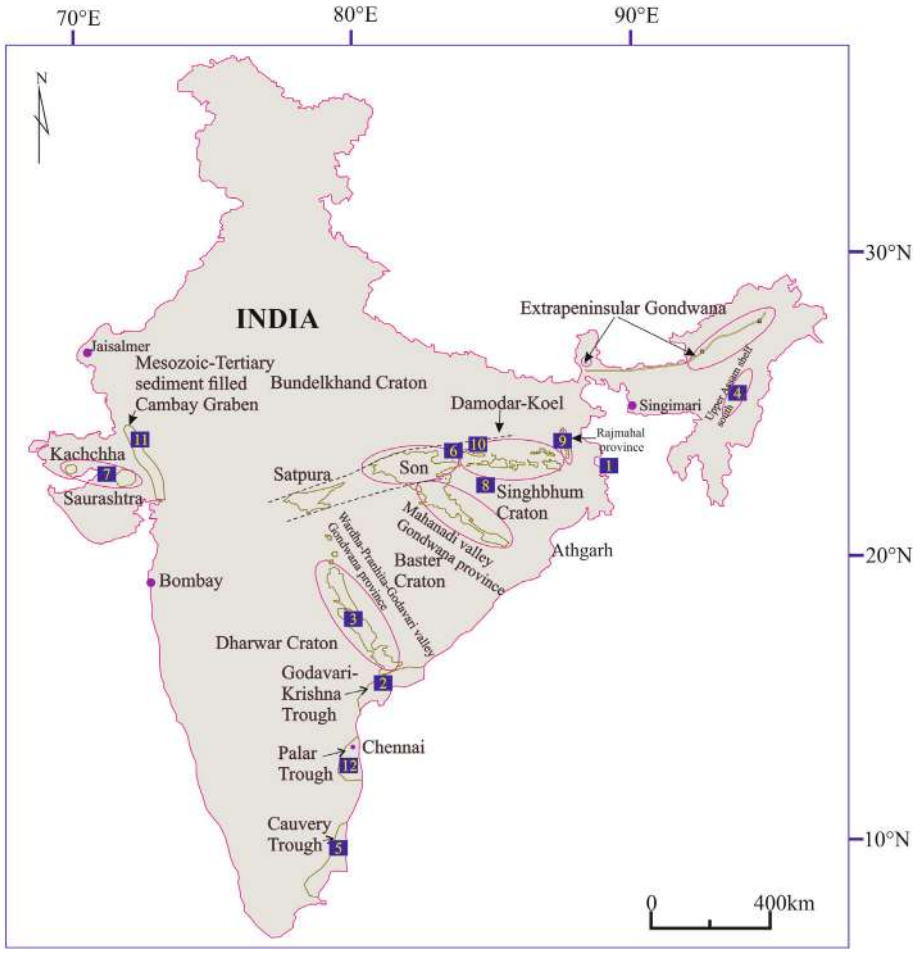

FIGURE 12 The Gondwana basins of India and hydrocarbon prospect (modified from Biswas, 1999; Mukhopadhyay, Mukhopadhyay, Roychowdhury, & Parui, 2010): (1) Bengal basin—Banerjee, Marak, and Biswas (2013); Phaye et al. (2013); Dwivedi (2016) (perspective with hydrocarbon shows (gas), (2) Krishna–Godavari Basin—Khan et al. (2000); Biswas et al (2003); Dwivedi (2016) (proven petroliferous basin), (3) Pranhita–Godavari-poorly explored—Dwivedi (2016), (4) Dhansiri valley-Assam-shows hydrocarbon (liquid and gas): Both lower and upper Gondwana—Das et al. (2004), (5) Cauvery Basin-proven petroliferous basin (oil and gas)—Dwivedi (2016), (6) Damodar and Son valley-coal bed methane—Singh, (2010); Dwivedi (2016), (7) Kutch-Saurashtra Basin-proven petroliferous basin (gas)—Chatterjee et al. (2020), (8) Karanpura coalfield, Jharkhand-hydrocarbon generation potential (oil and gas)—Singh & Jha (2018), (9) Rajmahal Basin: Indication of hydrocarbon generation in coal deposits—Singh & Singh (1994), (10) Auranga Basin: Hydrocarbon generation potential from Barakar Formation: Verma et al. (2018), (11) Cambay Basin–proven petroliferous basin—Dwivedi (2016). (12) Palar Basin-proven petroliferous basin—Biswas (2012)

Pradhan et al., 2013; Rajendran, Rajendran, Thulasiraman, Andrews, & Sherpa, 2011; Ravi Kumar, Hazarika, Prasad, Singh, & Saha, 2012). The NNE-trending and steeply west-dipping Gish transverse fault is the northern extension of the Malda-Kishanganj Fault. The seismic evidences suggest that the fault is continuing beneath the Himalaya between the Dharan salient and the Gurubathan recess in Sikkim and is highly seismogenic (De & Kayal, 2004).

Major shear component associated with MCT and DT zones documented in the field (top-to-SW) indicates an NNW-directed compression (Figure 2c). The direction of compression is in conformity with the tectonic stress in the present area deduced from stress tensor inversion (Baruah & Kayal, 2013). However, there are variations in the compression directions in NE India (indicating heterogeneous zones of transpression and transtension) as the Indian Plate subducted obliquely below the Burmese Plate (Baruah & Kayal, 2013). Because the region is tectonically complex, care must be taken in linking seismicity to different thrusts or strike-slip faults. Along the Bomdila Fault, the heterogeneity of the basement topography may reflect rotation of stress at sub-crustal depth below the brittle–ductile transition (~15 km, Fossen, 2016). It is possible that the plane of detachment or MHT is intersected by Bomdila Fault in the form of a lateral ramp dipping steeply to NE. This is inferred from the top-to-SSE shear in the Bomdila mylonitic gneiss where the shear planes dip steeply towards NE. Further, the intersection between the Bomdila Fault and the Himalayan Frontal Thrust (HFT) and the MBT may be studied keeping in mind the vulnerability of HFT and MBT in other parts of the Himalaya (Mukhopadhyay, Riguzzi, Mullick, & Sengupta, 2020).

6 | HYDROCARBON POTENTIAL OF GONDWANA SEDIMENTS

Table 4 presents a generalized stratigraphic succession of the north bank of the Brahmaputra River (Bharali, Gohain, & Sastri, 1999). The extra-peninsular Gondwana rocks occur in a linear belt extending along the MBT from Sikkim and Bhutan in the west up to the Pashighat of Arunachal Pradesh in the east (Figures 12 and 13). Along the Kameng River section, the Gondwana sediments cover a total area of ~690 km^2 and are divided into Bichom and Bhareli formations. The Bichom Formation consists of dark grey shale, clay shale, calcareous sandstone and diamictites indicating a marine facies. The Bhareli

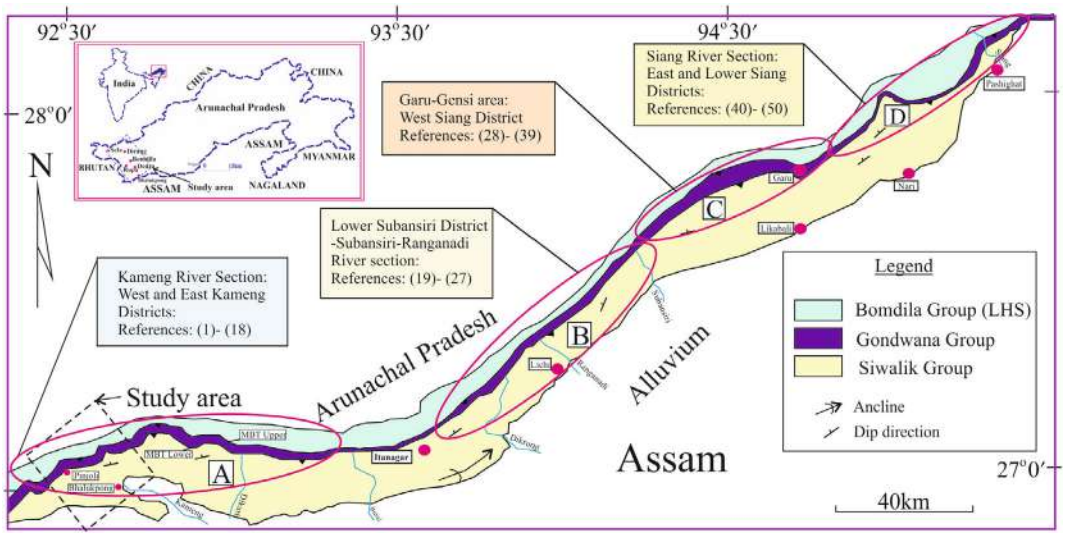

FIGURE 13 Gondwana Group of rocks in Arunachal Himalaya from Bhutan–Arunachal border in the west to Pashighat in the east (modified from Srinivasan, 2003). Geological survey of India started the mapping of the Gondwana outcrop in Arunachal Himalaya in the early 50s. We have given an account of the publications of the Gondwanas of Arunachal Himalaya. It is significant that a few workers analysed the Gondwana rocks for its hydrocarbon potential. The Gondwana mapping was mainly carried out in the four corridors (a: Kameng, b: Subansiri-Ranganadi, c: West Siang, and d: East and lower Siang). Majority of the publications cover two–three corridors for studies mainly in regard to palynostratigraphy, geochemistry and field disposition of rocks. Accordingly the publications are shown through four ellipses: (a): (1) Bhuyan et al. (2007), (2) Dutta (1980), (3) Dutta and Singh (1980), (4) Dutta, Srivastava, and Gogoi (1988), (5) Kumar (1997), (6) Acharya, Ghosh, Ghosh, and Shah (1975), (7) Acharyya (1983), (8) Ramachandran and Mallick (1976), (9) La touché (1885), (10) Singh (1983), (11) Verma and Tandon (1976), (12) Tiwari and Srivastava (2000), (13) Bhusan (1999), (14) Acharya et al. (1975), (15) Jain and Das (1973), (16) Sahini and Srivastava (1956), (17) Singh (1987), (18) Sinha and Mishra (1984). (b): (19) Laskar (1956), (20) Singh (1973), (21) Singh and Mathur (1982), (22) Diener (1905), (23) Tripathi and Roy Chowdhury (1983), (24) Laul, Mishra, and Shrivastava (1988), (25) Dutta, Gill, and Srinivasan (1983), (26) Acharyya et al. (1975), (27) Laskar (1954). (c) (28) Nayak et al. (2009), (29) Prakash et al. (1988), (30) Singh (2013), (31) Mahanta et al. (2017), (32) Mahanta et al. (2019), (33) Mahanta et al. (2020), (34) Mahanta et al. (2021), (35) Goswami et al. (2013) (36) Goswami, Baruah, et al. (2020), (37) GSI (2010), (38) Srivastava and Bhattacharya (1996), (39) Roy Chowdhury (1978), (d) (40) Jayprakash and Patel (1991), (41) Singh (1975), (42) Singh (1979), (43) Singh and Singh (1983), (44) Prasad, Dey, Gogoi, and Maithani (1989), (45) Sinha, Satsangi, and Mishra (1986), (46) Jayprakash et al. (1990), (47) Laskar (1954), (48) Laul, Khan, and Sinha (1986), (49) Roychowdhury and Sinha (1983), (50) Sinha and Mathur (1977)

Formation consists of alternating sequence of carbonaceous shale, coal, silt stone, and sandstone in the lower part which indicates a continental facies (Figure 14). These sediments occur as thrust slices/caught up materials in folds—between the Lesser Himalayan Bomdila Group of rocks in the north and Sub–Himalayan Siwalik Group in the south (Goswami et al., 2013; Goswami, Baruah, Mahanta, Kalita, & Borah, 2020). Parts of the Permian Gondwana rocks might stay concealed beneath the orogenic belts along the periphery of the upper Assam shelf (Nayak et al., 2004; Verma & Mukhopadhyay, 1977). Gondwana sediments in the Dhansiri valley SW of Bomdila Fault are encountered at different locations (Figure 1b). These sediments can be subdivided in to Lower Gondwana (Early Permian) consisting of predominantly sandstone with shale intercalations deposited in marine to fluvial set-up and Upper Gondwana (Early Cretaceous) composed of alternating sandstone and carbonaceous/coaly shale accumulated under shallow marine to fluvial conditions (Das, Sarma, & Ayyadurai, 2004).

Gondwanas of Arunachal Himalaya have been mapped by the Geological Survey of India in the early 50s. Since then, palynology, palynostratigraphy of the Gondwana sediments, and geochemistry of the Gondwana coals have been a major subject of study (Figure 13). However, detailed information on the (structural) geology of the Gondwana rocks in the eastern Himalaya has so far been scanty. This is revealed by the lack of mention of Arunachal Himalaya in any of the categories of basins as presented in the recent literatures (e.g., Biswas, 2012; Dwivedi, 2016 & Peters, Mahanti, & Singh, 2005). Bhandari (1983) categorized basins with the Gondwana rocks in India as the Category IV basin. Categoy IV basins are the ones which are 'either poorly explored or having inadequate geological information or are rated poor based on present concepts and knowledge of petroleum geology but considered prospective by analogy as compared to the similar basins in the world with proven prospects' (Biswas, 2012). Potter, Franca, Spence, and Caputo's (1995) global review on hydrocarbon prospect of Gondwana rocks, there is no mention of India. Dwivedi (2016) however referred Lesser Himalaya as a suitable location for further studies. In fact, Lesser Himalaya has been targeted for several isolated studies in the western Himalaya (Krol, Tal and Blaini formations of the Garhwal Inner Lesser Himalaya) (review in Bose & Mukherjee, 2020).

The Indian oil companies have been attempting basins with 'poor potential and high risk' (Bhoj, 2008). In that context the Gondwana rocks in the Arunachal Himalaya can be targeted for further studies, noting that the Gondwana rocks in India (Biswas, 2012; Dwivedi, 2016; review in Figure 12) and elsewhere (Potter et al., 1995) have been proved to be prospective for H-C exploration over the last two decades. Only Bhuyan, Rashidi, and Borah (2007) studied organic geochemistry and source rock potential of the Gondwana rocks in Arunachal Pradesh. They found that the rock has a good potential of having hydrocarbon in a gaseous form. Pahari, Singh, Prasad, Singh, and Bhandari (2008) expected oil shale from Gondwana sediments (gritty sandstones, carbonaceous shale, and coal lenticles) in Arunachal Pradesh (and also in Assam, Naganad and Manipur). Indian Gondwana rocks have a good potential for coal bed methane exploration (Dutt, 2008). The Permian and the Early Cretaceous Gondwana sediments in the transverse grabens formed in the Indian basement show good hydrocarbon indications in the Dhanisiri valley of Upper Assam shelf (SW of Bomdila Fault—Figure 1b) (Bhoktiary, Borah, Mathew, & Phukan, 2017; Mishra, Bhoktiari, Rahman, &

FIGURE 14 The Gondwana sequence in the footwall of Bome thrust in the Kameng River section, western Arunachal Himalaya (see Figure 2). (a) Sandstone, carbonaceous shale, and coal in the lower Gondwana Bhareli Formation, ~1 km east of the Pinjoli Nala and the highway crossing. (b) Coal beds within hard massive lower Gondwana sandstone ~2 km east of Pinjoli Nala. (c) Shear related folding in the lower Gondwana Bichom Formation near Sessa ~2 km north of Pinjoli. (d) The thrust contact of the rocks of the Bhareli Formation show fault gouge and carbonaceous shale (top right). The location is ~7.5 km from Pinjoli Nala. Maushumi Gogoi ~195 cm height standing, as a marker

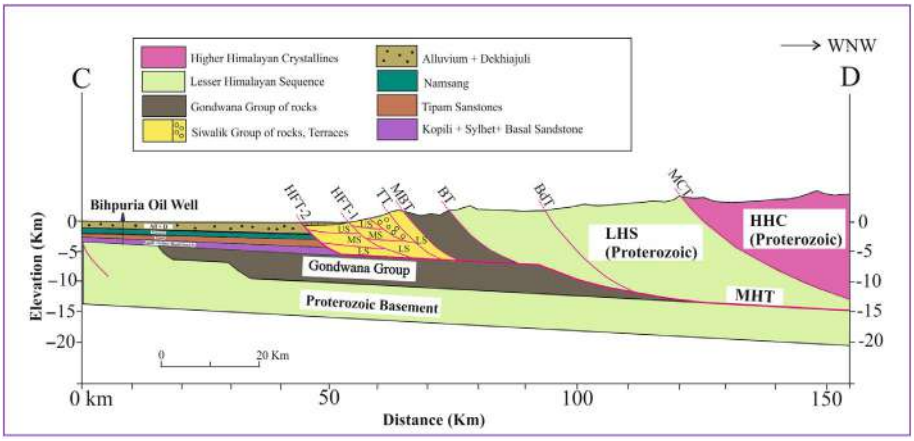

FIGURE 15 The cross-section along CD (see Figure 1b) (based on DeCelles et al., 2016; Yin et al., 2010b). The depth of the basement-after Kumar and Borgohain (2005). The Gondwana is shown in the underthrusted Indian basement in the north

Rahaman, 2016; Naik, 2001; Naik, Kumar, & Soren, 2004). These sediments above the basement can act as independent petroleum system below the Tertiary sediments of the Upper Assam valley.

Detail textural studies of the Gondwana rocks in Arunachal Pradesh indicated that the sediments were deposited in a marine condition, where transgression and regression persisted (Bhuyan & Borgohain, 2013; Mahanta, Sarmah, & Goswami, 2019). In other works, swampy-marginal environment (Prakash, Singh, & Srivastava, 1988), a passive margin tectonic setting (Mahanta, Syngai, Sarmah, Goswami, & Kumar, 2020), a lagoonal environment (Mahanta et al., 2021) have been deciphered for the Gondwana rocks in the Arunachal Himalaya. These environments of deposition are promising in terms of the presence of a hydrocarbon reservoir. The-concealed Gondwana rocks in the down-faulted basement of the upper Assam shelf as well as the under-thrust basement beneath the orogenic belt (the Himalaya and the Naga orogen), are presumed to be the 'source kitchen' under deeper burial condition and generated hydrocarbon, which have migrated and redistributed in the suitable structures developed in the Upper Assam foreland basin owing to thrust loading during the post-Oligocene (Naik, 2001; Naik et al., 2004). Otherwise it is difficult to explain the source rock for the petroleum system in the Upper Assam foreland basin as the existing source rocks, namely, Sylhet limestone, Kopili shale, Barail coal–shale litho units might be immature as evidenced by the reported low vitrinite reflectance value of 0.5%, low TTI value (0.56–343.3) and low transformation ratio of 0.28 (Naik, 2001; Naik et al., 2004). Therefore, only the deepest part of the basin locally may form oil window zone with high reflectance values, TTI and transformation ratio as mentioned above. It may be suggested that a critical analysis is further required to study the Gondwana sediments on the backdrop of the tectonic setup of north-east India.

Gondwana sediments in the Dhansiri valley show good hydrocarbon indications which can act as an independent petroleum system where source, reservoir, cap, and entrapment exists in deeper part of the grabens in the basement. The sediments exhibit migratory bitumen with TAI value 2.5 and P.I. 0.41 (Nayak, Singh, Upadhyay, & Bhattacharyya, 2009). Moreover, the TOC ranges from 0.58 to 0.73 and the hydrogen Index ranges from 8 to 95 (Nayak et al., 2009).

Considering a long-distance under-thrusting of the Permian and Tertiary strata below the Bome and the MBT-Lr, we have prepared a structural section a CD line (Figures 1b and 15—modified from DeCelles et al., 2016; Yin et al., 2010b). The steepening of the detachment at the top of the footwall ramp is not considered. Along the section, the Gondwana sequence may extend to the north of the Bihpuria Oil Well in the north bank of the Brahmaputra (Kumar & Borgohain, 2005).

Narayanan (2005) emphasized the role of field-based studies in discovering oil in the present time where geophysical techniques are dominating the field. In this article with field data from the Gondwana rocks, we suggest that these Gondwana sediments can be explored in the underthrust basement below the Himalaya due to their deeper burial during thrust loading. Further, these sediments may be explored in the down-faulted basement in the east of Bomdila Fault beneath the orogenic belts.

In the upper Assam shelf the sediment thickness is low (~5 km) and the velocity variation pattern of the seismic waves matches with the depth trend of the basement (Mandal, Chakraborty, & Dasgupta, 2011). We interpret that in the south of the Bomdila Fault, the Gondwana beds in the MBT footwall remain flat without further deformation and are to be investigated further for hydrocarbon potential.

7 | DISCUSSION

Structural analysis of the LHS and HHC across DT and MCT zones reveals significant imprints of deformation. Ductile shear fabrics in the thrust zones depict a top-to-SW shear. Abrupt swing in the trace of the MCT from NE to NNW created a salient in the MCT. Further, the NNW-trending segment of the salient is parallel to the top-to-SSE shear in the mylonitic Bomdila Gneiss. The salient in the MCT may be due to the WNW-trending Bomdila Fault. This is because the MCT salient in Sikkim and Bhutan are interpreted to be due to the northern extension of the basement faults like Tista and Kopili faults (e.g., Acharyya, 1971; Mitra et al., 2010). Both Kopili and Bomdila Faults are transverse basement faults extending from the belt of Schuppen to MCT in Himalaya. Both the Kopili and Bomdila faults are highly seismogenic. On this backdrop, a detail structural analysis of the

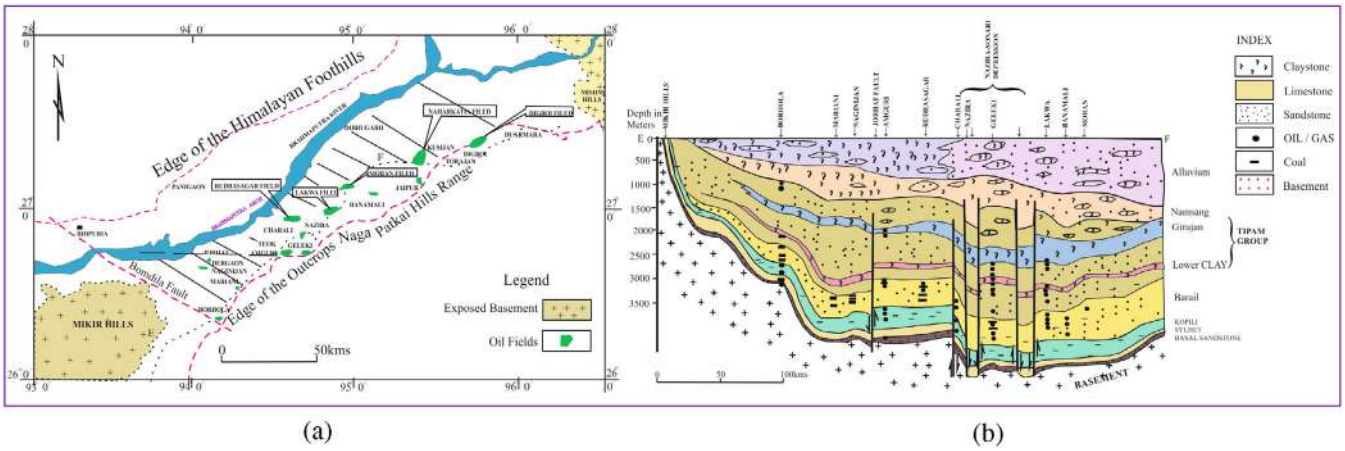

FIGURE 16 Configuration of the upper Assam Shelf in the east of Bomdila Fault. (a) The map shows the position of oil fields in upper Assam (modified from Desikachar, 1984). (b) The faulted basement east of Bomdila Fault. The older sediments consist of Gondwanas in faulted troughs and marine Cretaceous sediments. The overlying sediments consist of complete Tertiary and younger sediments (Desikachar, 1984)

mesoscopic field structures was carried out to constrain the correlation of the outcrop-scale structures to the regional structural framework.

In the internal domain of the orogen, the concentration of shear strain is manifested by ductile shear zones and mylonitic structures (Mukherjee, 2013; Wojtal & Mitra, 1988). In the MCT ductile shear zone at Seppar we have noticed the tightening of the folds with top-to-SW shear (Figure 6d). The late shear is indicated by the tightening of the folds in the direction of shear (Figure 6d) (Mukherjee et al., 2015). The orogen transverse close to tight F1and F2 folds plunge moderate to steeply to the NW or SE direction in the lower structural horizon of DT (400 m north of the Munna camp). These folds have a vergence towards SW (Figure 7b,c). The NE to SW directed orogen-parallel shear may be synchronous or overprinted the D2 ductile deformation along the thrust zones of MCT and DT. Orientation of the minor structures in MCT and DT zones indicates their progressive reorientation parallel to the map-scale faults (MCT and DT).

We may also interpret that MCT and DT moved synchronously if the MCT hanging wall never separated from the footwall and the northern Indian craton (Martin, 2016). The coeval ductile shear in the MCT and DT zone thus indicate a thrust-parallel top-to-SW shear and all evidences point towards ductile shear during the D2 phase of deformation. The synchronous ductile shear in the MCT and DT zones thus indicate a thrust parallel top-to-SW shear. The pervasive ductile shearing during D2 phase of deformation is also imprinted in the northern part of Bomdila gneisses as top-to-SE shear (Bikramaditya et al., 2017). The footwall ramp interpreted across the LHS is observed to be roughly parallel to the seismogenic Bomdila Fault (DeCelles et al., 2016) (Figures 1b and 2d).

The Bomdila Fault, in its ESE extension to the Belt of Schuppen, separates the Mikir Massif from the Upper Assam Shelf. The fault dips steeply to the NE direction and the down thrown basement in the Upper Assam Shelf is shown in Figure 16a,b (modified from Desikachar, 1984). Thus, the Precambrian basement rocks exposed in the Shillong-Mikir (Karbi-Anglong) Massif constitute the-floor of the Upper Assam Basin over which the sedimentary pile belonging to the Gondwana Group and Upper Cretaceous–Tertiary Period were accumulated with variable thickness. Significantly, ~ 94°E longitude, gravity contours of −80 to −180 m Gals take a sharp southward turn along the main edge of the Karbi-Anglong Massif with steep gradient (Figure 17a).

The Gondwana sediments deposited in the transverse grabens in the down-faulted basement of the upper Assam Shelf may be the source rock for the hydrocarbon under deeper burial conditions. The formation of the rifts in the Indian craton and sedimentation in the graben might have taken place during the break-up and northward drift of the Indian Plate during Jurassic-Early Cretaceous Period (Biswas, 1999). These sediments in the southwest of upper Assam Shelf, interpreted as syn-rift-fill from the seismic data, show good indication for hydrocarbon generation. These 38–389 m thick sediments are overlain by 34–74 m thick basaltic trap-rocks (Bhoktiary et al., 2017). The sediments experienced post-Gondwana uplift along with the Mikir Massif. Towards north and south-east, the sediments deformed presumably beneath the adjoining Himalayan and the Naga orogenic belts (Bhoktiary et al., 2017).

In the northern part of the Upper Assam valley, the basement slopes down to the Himalayan foothills with a gravity low around North Lakhimpur (27°14′N:94°06′E), where the basement lies at 5.5 km with thick cover sediments. It may be speculated that parallel to the Bomdila Fault, the down-throw of the basement is inhomogeneous across the Brahamputra fracture. In the Mishmi Hills part, the basement goes deeper towards northeast with thick pile of Tertiary sediments along with the Mesozoic and Gondwana rocks (Verma & Mukhopadhyay, 1977). The continuation of the Bomdila Fault under the Himalayan orogen is visualized as in Figure 17b.

The geologic cross-sections along the Bhalukpong–Zimithang traverse show possibilities for a north-dipping ramp in the MHT (Yin et al., 2010b). Significantly, the Early-Middle Miocene deformation in HHC is entirely ductile, whereas that in the LHS in Late Miocene–Pliocene is generally brittle, which involves the foreland—propagation of the upper crustal rocks (Searle et al., 2017). It is noteworthy that below the depth of the brittle—ductile transition zone (~15 km) the

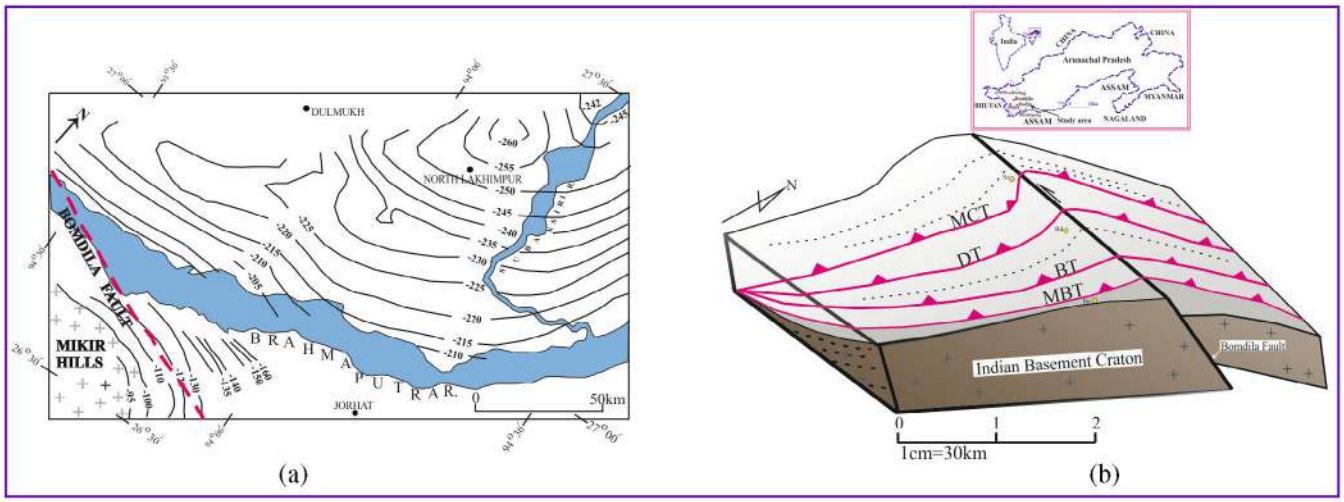

FIGURE 17 (a) Bouger gravity anomaly in the east of Mikir Massif and Bomdila Fault (modified from Nandy, 2001). Gravity anomaly contour (−260 mGal) in the north showing North Lakhimpur low. (b) Cartoon showing Bomdila Fault in the Indian basement under the Himalayan orogen. The recess in the MCT and DT shown prominently in the north

change in the stress is reflected through the heterogeneity of the basement topography. It is possible that the plane of detachment (MHT) is intersected by the Bomdila Fault in the form of a lateral ramp dipping very steeply to the NE direction. As the deeper (>~20 km) motions were accommodated by ductile shear, any earthquake that originated near the 20 km zone can propagate through 15–20 km of the crust through brittle foreland propagating thrusting (Searle et al., 2017). From this perspective, the cluster of earthquakes in the NW of Bomdila Fault needs a detailed study regarding the major earthquake in the region. The compression axis map (Figure 1c) shows an ongoing ~N-S compression in the area. Therefore, major earthquakes can affect the oil-fields in the Brahmaputra valley.

Focal mechanism solutions indicate strike-slip movement in Kopili and Bomdila faults. It is further observed that the focal depth of the bulk of the earthquake originated around ~20 km (brittle-ductile transition zone) and propagates through the brittle foreland vergent thrusts. Considering this aspect, the frontal shallower thrusts (MFT and it splays) may become vulnerable and need indepth study as studied in other segments of Himalaya.

8 | CONCLUSIONS

1. In the western Arunachal Himalaya, the ductile shear fabrics in the MCT and DT zones depict top-to-SW shear. This shear sense is parallel to the cusp or salient of the MCT trace seen in the map scale.
2. Ductile shear fabrics in the mylonitic Bomdila Gneisses depict a top-to-SE shear, which is parallel to the southern trace of the cusp in the map scale as well as the orientation of the WNW trending Bomdila Fault.
3. Garnet inclusion trail geometry in the metapelites of the Dirang Formation indicates reversal of shear sense towards the DT zone. This depicts a late or post D2 reactivation of ductile shear and may be synchronous with the formation of cusp or salient in MCT.
4. The focal mechanism solution of the earthquake events indicates that the NW of the Bomdila Fault is seismogenic. The fault separates the Shillong–Mikir Massif from the Upper Assam Shelf. There may be number of synthetic faults in the basement with a variable throw across the Brahmaputra fracture. Surface signatures of the MCT and DT zone indicate exhumed ductile deformation below the brittle-ductile transition zone. The present study links the surface deformation due to ductile shear and signatures of underthrusting of the deformed Indian basement with the regional seismicity. Further, the focal depths of the recent earthquake events in the zone callfor a detailed study of motions originating near the 20 km zone of ductile deformation, which may propagate through the upper 15–20 km of the crust in the form of brittle thrusts propagating towards the foreland.
5. The SE or ESE extension of the marine Gondwana sediments in the transverse grabens in the underthrusted basement may be explored for hydrocarbon traps. Gondwana sediments of the Dhansiri valley of south Assam shelf show good hydrocarbon indications. This study suggests exploration of the hydrocarbon-bearing marine Gondwana sediments. These sediments underwent deeper burial during thrust loading beneath the Himalaya. The study further highlights the exploration for Gondwana sediments in the down-faulted basement in the east of Bomdila Fault beneath the Upper Assam Shelf and Naga-Patkai orogen.

ACKNOWLEDGEMENTS

Tapos Kumar Goswami and Mousumi Gogoi received financial assistance from International Geological Congress Secretariat, New Delhi (IGC-2020), sanction no. 36th IGC Sectt./Field Trips/2018/20.29) for conducting the fieldwork for the traverse NER-001. Tapos Kumar Goswami and Pranjit Kalita thank their

Head of the Department for providing facilities to carry out the lab work. Bashab Nandan Mahanta, Ramesh Laishram, Hiruj Saikia, and Bhaskar Oza are grateful to the Additional Director General, North-eastern Region, Geological Survey of India, Shillong for the permission to publish the work. CPDA grant (IIT Bombay) supported Soumyajit Mukherjee. We thank the Chief Editor Ian Somerville, Handling Editor A. K. Singh, and the reviewers for providing detailed review comments.

CONFLICT OF INTEREST

The authors declare no potential conflict of interest.

DATA AVAILABILITY STATEMENT

The data that support the findings of this study are available from the corresponding author upon reasonable request.

ORCID

Tapos Kumar Goswami https://orcid.org/0000-0003-4489-597X
Soumyajit Mukherjee https://orcid.org/0000-0003-2247-8526
Bashab Nandan Mahanta https://orcid.org/0000-0002-6546-1575
Mousumi Gogoi https://orcid.org/0000-0003-1319-9226

REFERENCES

Acharya, S. K., Ghosh, S. C., Ghosh, R. N., & Shah, S. C. (1975). The continental Gondwana Group and associated marine sequence of Arunachal Pradesh (NEFA), eastern Himalaya. *Himalayan Geology*, *5*, 60–82.

Acharyya, S. K. (1971). Structure and stratigraphy of the Darjeeling frontal zone, eastern Himalaya. In *Recent geological studies in the Himalaya* (Vol. 24, pp. 71–90). Kolkata: Geological Survey of India Miscellaneous Publication

Acharyya, S. K. (1983). *Geological framework of the Eastern Himalayas in part of Kameng, Subansiri, Siang districts, Arunachal Pradesh* (Vol. 43, pp. I45–I5Z). Shillong, ML: Geological Survey of India Miscellaneous Publication.

Aerden, D. (1998). Tectonic evolution of the Montagne Noire and a possible orogenic model for syncollisional exhumation of deep rocks, Variscan belt, France. *Tectonics*, *17*, 62–79.

Banerjee, B., Marak, I. A., & Biswas, A. K. (2013). Subcrop Gondwana of Bengal Basin and their reservoir characteristics. *Journal of Geological Society of India*, *81*, 32–754.

Baruah, S., & Kayal, J. (2013). State of tectonic stress in Northeast India and adjoining South Asia region: An appraisal. *Bulletin of Seismological Society of America*, *103*, 894–910. https://doi.org/10.1785/0120110354.

Baruah, S., Saikia, S., Baruah, S., Bora, P. K., Tatevossian, R., & Kayal, J. R. (2016). The September 2011 Sikkim Himalaya earthquake Mw 6.9: Is it a plane of detachment earthquake? *Geomatics, Natural Hazards and Risk*, *7*(1), 248–263. https://doi.org/10.1080/19475705.2014.895963.

Bell, T., Rubenach, M., & Fleming, P. (1986). Porphyroblast nucleation, growth and dissolution in regional metamorphic rocks as a function of deformation partitioning during foliation development. *Journal of Metamorphic Geology*, *4*, 37–67.

Biswas, S. K. (2003). Regional tectonic framework of the Pranhita–Godavari basin, India. *Journal of Asian Earth Sciences*, *21*, 543–551.

Bhandari, L. L. (1983). Introduction. In L. L. Bhandari, B. S. Venkatachala, P. Mitra, R. Kumar, D. C. Srivastava, & S. N. Swamy (Eds.), *Petroliferous basins of India*. Dehradun: KDMIPE, ONGC.

Bharali, B., Gohain, K., & Sastri, P. S. S. (1999). *A re-look into geology and hydrocarbon prospects of north bank of Brahmaputra River, Upper Assam Basin, India*. Paper presented at Proceeding 3rd International Petroleum Conference and Exhibition PETROTECH, New Delhi (pp. 25–30).

Bhattacharya, S., & Nandy, S. (2007). Geology of the Western Arunachal Himalaya in parts of Tawang and west Kameng districts, Arunachal Pradesh. *Journal of Geological Society of India*, *72*, 199–207.

Bhoj, R. (2008). Fathoming unexplored terrain. *Association of Petroleum Geologists Bulletin*, *2*, 77–82.

Bhoktiary, P., Borah, R., Mathew, R., & Phukan, J. (2017). Syn-Rift sediments and its significance for hydrocarbon exploration in and around southern part of upper Assam Shelf. *Assam & Assam Arakan Basin, India, ONGC Bulletin.*, *52*(2), 149–157.

Bhusan, S. K. (1999). Reappraisal of the geology between the MBF and the MCT in western Arunachal Pradesh. In P. K. Verma (Ed.), *Geological studies in the Eastern Himalayas* (pp. 161–176). Delhi: Pilgrim Books Pvt. Ltd..

Bhuyan, D., & Borgohain, P. (2013). Palynodebris analysis and palynological approach to depositional environment of the Permian Gondwana rocks of West Kameng District, Arunachal Himalayas. *Journal of Earth Science, Special*, 247–252.

Bhuyan, D., Rashidi, W. S., & Borah, B. (2007). Organic geochemistry and source rock potential of Gondwana rocks of Kameng district, Arunachal Pradesh. *Journal of SCTU*, *3*, 122–140.

Bikramaditya, R. K., Chung, S., Singh, A. K., Lee, H. Y., & Lemba, L. (2021). Zircon U–Pb ages and Hf isotopes of I-type granite from western Arunachal Himalaya, NE India: Implications for the continental arc magmatism in the Palaeoproterozoic supercontinent Columbia. *Geological Journal*. https://doi.org/10.1002/gj.4342.

Bikramaditya, R. K., & Gururajan, N. S. (2011). Microstructures in quartz and feldspars of the Bomdila Gneiss from western Arunachal Himalaya, Northeast India: Implications for the geotectonic evolution of the Bomdila mylonitic zone. *Journal of Asian Earth Sciences*, *42*(6), 1163–1178.

Bikramaditya, R. K., Sen, K., & Sangode, S. J. (2017). Detection of a weak late-stage deformation event in granitic gneissthrough anisotropy of magnetic susceptibility: Implications for tectonic evolution of the Bomdila Gneiss in the Arunachal Lesser Himalaya. *Northeast India. Geological Magazine*, *15*(3), 476–490.

Biswal, T. K. (1997). Structural contrasts across the Main Central Thrust in Bhutan Himalaya. *Himalayan Geology*, *18*, 113–117.

Biswas, S. K. (1999). A review of the evolution of rift basins in India during Gondwana with special reference to western Indian basins and their hydrocarbon prospects. *PINSA*, *65*(3), 261–283.

Biswas, S. K. (2012). Status of petroleum exploration in India. *Proceedings of the National Academy*, *78*, 475–494.

Bollinger, L., Avouac, J.-P., Beyssac, O., Catlos, E. J., Harrison, T. M., Grove, M., … Sapkota, S. (2004). Thermal structure and exhumation history of the Lesser Himalaya in Central Nepal. *Tectonics*, *23*, TC5015. https://doi.org/10.1029/2003TC001564.

Bose, N., & Mukherjee, S. (2019). Field documentation and genesis of the back-structures from the Garhwal Lesser Himalaya, Uttarakhand, India. In R. Sharma, I. M. Villa, & S. Kumar (Eds.), *Crustal architecture and evolution of the Himalaya-Karakoram-Tibet Orogen* (Vol. 481, pp. 111–125). London: Geological Society of London Special Publications.

Bose, N., & Mukherjee, S. (2020). Estimation of deformation temperatures, flow stresses and strain rates from an intra-continental shear zone: The Main Boundary Thrust, NW Himalaya (Uttarakhand, India). *Marine and Petroleum Geology*, *112*, 104094.

Chatterjee, D., Mohanty, P. R,. & Singh, S. (2020). Exploring sub-basalt reservoirs using object-oriented imaging: A case study from Kutch–Saurashtra area, India. *Journal of Earth System Science*, *129*, 158.

Curray, J. R. (2014). The Bengal depositional system: From rift to orogeny. *Marine Geology*, *352*, 59–69. https://doi.org/10.1016/j.margeo.2014.02.001.

Daniel, C. G., Hollister, L. S., Parrish, R. R., & Grujic, D. (2003). Exhumation of the Main Central Thrust from lower crustal depths, eastern Bhutan Himalaya. *Journal of Metamorphic Geology*, *21*, 317–334.

Das, A. K., Bakliwal, P. C., & Dhoundial, D. P. (1975). *A brief outline of the geology of parts of Kameng district, NEFA* (Vol. 24(1), pp. 115–127). Shillong, ML: Miscellaneous Publication of Geological Survey of India.

Das, K. C., Sarma, V. S. B., & Ayyadurai, M. (2004). *Gondwana sediments: A promising hydrocarbon exploration target in Assam shelf*. Paper presented at 5th Conference & Exposition on Petroleum Geophysics, Hyderabad, India. (pp. 468–472).

Dasgupta, S., Mukhopadhyay, B., & Mukhopadhyay, M. (2013). Role of transverse tectonics in the Himalayan collision: Further evidences from two contemporary earthquakes. *Journal of Geological Society of India*, *81*, 241–247.

Dasgupta, S., Mukhopadhyay, M., & Nandy, D. R. (1987). Active transverse features in central portion of the Himalaya. *Tectonophysics*, *136*, 255–264.

De, R., & Kayal, J. R. (2004). Seismic activity at the MCT in Sikkim Himalaya. *Tectonophysics*, *386*, 243–248.

DeCelles, P. G., Carrapa, B., Gehrels, G. E., Chakraborty, T., & Ghosh, P. (2016). Along-strike continuity of structure, stratigraphy, and kinematic history in the Himalayan thrust belt: The view from Northeastern India. *Tectonics*, *35*(12), 2995–3027.

DeCelles, P. G., Robinson, D. M., & Zandt, G. (2002). Implications of shortening in the Himalayan fold-thrust belt for uplift of the Tibetan Plateau. *Tectonics*, *21*, 10–62. https://doi.org/10.1029/2001TC001322.

Desikachar, S. V. (1984). Oil gas deposits in the deltaic sequence of sediments in the Cambay basin and Upper Assam valley in India. *Journal of Geological Society of India*, *25*(4), 199–219.

Diehl, T., Singer, J., Hetényi, G., Grujic, D., Clinton, J., Giardini, D., & Kissling, E. (2017). Seismotectonics of Bhutan: Evidence for segmentation of the Eastern Himalayas and link to foreland deformation. *Earth and Planetary Science Letters*, *471*, 54–64.

Diener, C. (1905). Notes on Anthracolithic fauna from the mouth of Subansiri gorge. *Records of the Geological Survey of India*, *32*(3), 189–198.

Dikshitulu, G. R., Pandey, B. K., Krishna, V., & Raju, R. (1995). Rb-Sr systematics of granitoids of the Central Gneissic Complex, Arunachal Himalaya: Implications on tectonism, stratigraphy and source. *Journal of the Geological Society of India*, *45*, 51–56.

Ding, L., Zhong, D., Yin, A., Kapp, P., & Harrison, M. (2001). Cenozoic structural and metamorphicevolution of the eastern Himalayan syntaxis (Namche Barwa). *Earth and Planetary Science Letters*, *192*, 423–438.

Duta, D., & Mukherjee, S. (2021). Extrusion kinematics of UHP terrain in a collisional orogen: EBSD and microstructure-based approach from the Tso Morari Crystallines (Ladakh Himalaya). *Tectonophysics*, *800*, 228641.

Dutt, A. B. (2008). Coal rank and CBM potentiality of Indian Gondwana basins. *Association of Petroleum Geologists Bulletin*, *3*, 101–110.

Dutta, S. K. (1980). Palynostratigraphy of the sedimentary formations of the Arunachal Pradesh. 2. Palynology of the siwalik equivalent rocks of Kameng District. *Geophytology*, *10*, 5–13.

Dutta, S. K., Gill, G. K. S., & Srinivasan, J. (1983). *Geology of the Subansiri and Kamala valleys*. Paper presented at Proceedings of Symposium on Geology and Mineral Resources of North eastern Himalayas, Geological Survey of India Miscellaneous Publication, *43*, 9–14

Dutta, S. K., & Singh, H. P. (1980). *Palynostratigraphy of the sedimentary formations of Arunachal Pradesh-I*. Paper presented at Proceeding of 4th International Palynological Conference, B.S.I.P. Lucknow, II, 617–626.

Dutta, S. K., Srivastava, S. C., & Gogoi, D. (1988). Palynology of the Permian sediments in Kameng district, Arunachal Pradesh. *Geophytology*, *18*(1), 53–61.

Duvall, M., Waldron, J. W. F., Godin, L., & Najman, Y. (2020). Active strike-slip faults and an outer frontal thrust in the Himalayan foreland basin. *Proceedings of the National Academy of Sciences*, *117*(30), 17615–17621.

Dwivedi, A. K. (2016). Petroleum exploration in India—A perspective and Endeavours. *Proceedings of the Indian National Science Academy*, *82*, 881–903.

Ellis, M. A., & Dunlap, W. J. (1988). Displacement variation along thrust faults: Implications for the development of large faults. *Journal of Structural Geology*, *10*, 183–192.

Fossen, H. (2016). *Structural geology* (p. 524). Cambridge: Cambridge University Press.

Gahalaut, V. K., & Kundu, B. (2012). Possible influence of subducting ridges on the Himalayan arc and on the ruptures of great and major Himalayan earthquakes. *Gondwana Research*, *21*, 1080–1088.

Gansser, A. (1964). *Geology of the Himalayas*. London/New York/Sydney: Interscience Publishers; John Wiley & Sons Ltd.

Gibson, R., Godin, L., Kellett, D. A., Cottle, J. M., & Archibald, D. (2016). Diachronous deformation along the base of the Himalayan metamorphic core, west central. *GSA Bulletin*, *128*(5–6), 860–878. https://doi.org/10.1130/B31328.1.

Godin, L., & Harris, L. B. (2014). Tracking basement cross-strike discontinuities in the Indian crust beneath the Himalayan orogen using gravity data—Relationship to upper crustal faults. *Geophysical Journal International*, *198*, 198–215.

Godin, L., Roche, R. S., Waffle, L., & Harris, L. B. (2018). *Influence of inherited Indian basement faults on the evolution of the Himalayan Orogen* (Vol. 481, pp. 251–276). London: Geological Society of London, Special Publication. https://doi.org/10.1144/SP481.4.

Goswami, S. B., Bhowmik, S., & Dasgupta, S. (2009). Petrology of a non-classical Barrovian inverted metamorphic sequence from the western Arunachal Himalaya, India. *Journal of Asian Earth Sciences*, *36*, 390–406.

Goswami, S. B., Bhowmik, S., Dasgupta, S., & Pant, N. (2014). Burial of thermally perturbed Lesser Himalayan mid-crust: Evidence from petrochemistry and P-T estimation of the western Arunachal Himalaya, India. *Lithos*, *208-209*, 298–311.

Goswami, T. K., Baruah, S., Mahanta, B. N., Kalita, P., & Borah, P. (2020). Thrust shear sense and shear zone fabrics in Higher Himalaya, Siyom valley, Eastern Arunachal Himalaya, India. *Journal of Geological Society of India*, *96*, 447–457.

Goswami, T. K., Bezbaruah, D., Mukherjee, S., Sarmah, R. K., & Jabeed, S. (2018). Structures and morphotectonic evolution of the frontal fold–thrust belt, Kameng river section, Arunachal Himalaya, India. *Journal of Earth System Science*, *127*(88), 1–11.

Goswami, T. K., Mahanta, B. N., Mukherjee, S., Syngai, B. R., & Sarmah, R. K. (2020). Orogen transverse structures in the eastern Himalaya: Dextral Riedel shear along the Main Boundary Thrust in the Garu-Gensi area (Arunachal Pradesh, India), implication in hydrocarbon geoscience. *Marine and Petroleum Geology*, *114*, 104242. https://doi.org/10.1016/j.marpetgeo.2020.104242.

Goswami, T. K., Sarmah, R. K., Mahanta, B. R., Syngai, B. R., Das, T., Ghosh, S., & Borgohain, B. (2013). Deformation at lateral ramps of the propagating thrust sheet: Examples of the nature of Main Boundary Thrust in some parts of West Siang District, Arunachal Pradesh, India. *South East Asian Journal of Sedimentary Basin Research*, *1*(2), 61–67.

GSI (2010). Geology and mineral resources of Arunachal Pradesh. Geological Society of India, Miscellaneous Publication, 30, IV I (i), Arunachal Pradesh.

GSI, Dasgupta, S., Pande, P., Ganguli, D., & Iqbal, Z. (2000). *Seismotectonic atlas of India and its environs, Spl. Pub. Series 59*. Kolkata: Geological Survey of India (P. L. Narula, S. K. Acharyya, & J. Banerjeee (Eds.)).

Heim, A., & Gansser, A. (1939). *Central Himalayas—Geological observations of the Swiss Expedition of 1936*. Denkschr. Schweiz. Naturf. Ges., *32*, 1–245.

Hodges, K. V. (2000). Tectonics of the Himalaya and southern Tibet from two perspectives. *Geological Society of America Bulletin*, *112*(3), 324–350.

Hossain, M. S., Khan, M. S., Abdullah, R., & Mukherjee, S. (2021). Late Cenozoic transpression at the plate boundary: Kinematics of the eastern segment of the Dauki Fault Zone (Bangladesh), and tectonic evolution of the petroliferous NE Bengal basin. *Marine and Petroleum Geology*, *131*, 106133.

Hu, X., Garzanti, E., Wang, J., Huang, W., An, W., & Webb, A. (2016). The timing of India-Asia collision onset–facts, theories, controversies. *Earth Science Review*, *160*, 264–299.

Ilg, B., & Karlstrom, K. (2000). Porphyroblast inclusion trail geometries in the Grand Canyon: Evidence for non-rotation and rotation? *Journal of Structural Geology*, *22*, 231–243.

Jain, A. K., & Das, A. K. (1973). On the discovery of Upper Palaozoic bryozoans from Kameng district, Arunachal Pradesh. *Current Science*, *42*(10), 352–355.

Jain, A. K., Singh, S., & Manickavasagam, R. M. (2002). Himalayan collisional tectonics, Gondwana research Group memoir no. 7. Field science, Hashimoto, 4.

Jayprakash, A. V., & Patel, S. K., (1991). Geolgy of the area around Pasighat, Ledum and Koya, E. Siang district, Arunachal Pradesh. Unpublished Programme Report, Geological Society of India.

Jayprakash, A.V., Singh, H. J. M., Panduranga, R., Sengupta, C. K., Patel, S. K., & Bora, A. (1990). Geology of the area around Pasighat, Koyu, Likhabali, Garu and Geru area, East & West Siang districts, Arunachal Pradesh (in 3 parts). Unpublished Programme Report, Geological Society of India, FS 1989–90.

Kayal, J. R. (2001). Microearthquake activity in some parts of Himalaya and the tectonic model. *Tectonophysics*, *339*, 331–351.

Kayal, J. R., Arefiev, S., Baruah, S., Hazarika, D., Gogoi, N., Gautam, J. L., … Tatevossian, R. (2012). Large and great earthquakes in the Shillong plateau–Assam valley area of Northeast India region: Pop-up and transverse tectonics. *Tectonophysics*, *532–535*, 186–192.

Kayal, J. R., Arefiev, S. S., Baruah, S., Tatevossian, R., Gogoi, N., Sanoujam, M., … Borah, D. (2010). The 2009 Bhutan and Assam felt earthquakes (Mw 6.3 and 5.1) at the Kopili fault in the northeast Himalaya region. *Geomatics, Natural Hazards and Risk*, *1*, 273–281.

Kellett, D. A., Cottle, J. M., & Larson, K. P. (2018). *The south Tibetan detachment system: History, advances, definition and future directions* (p. 483). London: Geological Society of London Special Publication. https://doi.org/10.1144/SP483.2.

Khan, M. S. R., Sharma, A. K., Sahota, S. K., & Mathur, M. (2000). Generation and hydrocarbon entrapment within Gondwanan sediments of the Mandapeta area, Krishna–Godavari basin, India. *Organic Geochemistry*, *31*, 1495–1507.

Kumar, G. (1997). *Geology of Arunachal Pradesh* (p. 217). Bangalore: Geological Society of India.

Kumar, M., & Borgohain, R. (2005). Palynofacies analysis and the depositional environment of Bihpuria well-A, North bank of Brahmaputra River, Upper Assam Basin. *Geological Society of India*, *65*, 70–82.

La touché. (1885). Notes on the geology of the Aka Hills, Assam. *Record of Geological Society of India*, *18*, 936–938.

Laskar, B. (1954). Geological Society of India Progress Report (unpublished)

Laskar. B. (1956). *On certain intercalations of rocks for oil with sub-Himalayan Gondwana*. Paper presented at Proceeding of Indian Science Congress, 43 Sess. 194.

Laul, V. P., Khan, A. S., & Sinha, N. K., (1986). Final report on Gondwana of Arunachal Pradesh. Unpublished Progress Report, Geological Society of India, FS 1984–85.

Laul, V. P., Mishra, U. K., & Shrivastava, S. C. (1988). Final report on Gondwana of Arunachal Pradesh. Unpublished Progress Report, Geological Society of India.

Le Fort, P. (1975). Himalayas, the collided range: Present knowledge of the continental arc. *American Journal of Science*, *275A*, 144.

Mahanta, B. N., Sarmah, R. K., & Goswami, T. K. (2019). Elucidation of provenance, palaeoclimate and tectonic setting of the Gondwana sandstones of Arunachal Himalayas. *Journal of Geological Society of India*, *94*(3), 260–266. https://doi.org/10.1007/s12594-019-1305-7.

Mahanta, B. N., Sekhose, K., Goswami, T. K., Vitso, V., Sarmah, R. K., Kumar, A., & Kumar, R. (2021). Depositional setup of the faunal coal balls from Bichom Formation of Lower Gondwana Group of Arunachal Himalaya: Insights from EPMA and Raman spectroscopy. *Journal of Sedimentary Environments.*, *6*, 159–168. https://doi.org/10.1007/s43217-020-00042.

Mahanta, B. N., Syngai, B. R., Sarmah, R. K., Goswami, T. K., Guha, S. K., & Kumar, A. (2017). Major oxide studies of Lower Gondwana coals, West Siang District, Arunachal Pradesh, India: Analysis of palaeo environment and depositional milieu. *Indian Journal of Geoscience*, *71*(2), 395–404.

Mahanta, B. N., Syngai, B. R., Sarmah, R. K., Goswami, T. K., & Kumar, A. (2020). Geochemical signatures of Lower Gondwana sandstones of eastern Arunachal Himalayas, India; implications for tectonic setting, provenance and degree of weathering. *Russian Journal of Earth Science*, *20*, 3–11. https://doi.org/10.2205/2020ES000698.

Mandal, K. L., Chakraborty, S., & Dasgupta, R. (2011). Regional velocity trend in Upper Assam Basin and its relations with basinal depositional history [Abstract]. *SEG Expanded Abstracts* (pp. 1222–1226). doi: https://doi.org/10.1190/1.3627423.

Martin, A. J. (2016). A review of definitions of the Himalayan Main Central Thrust. *International Journal of Earth Sciences.*, *106*, 2131–2145.

Mishra, S. K., Phukon, J. Y., Bhoktiari, P. R., & Rahaman, A. (2016). Integrated structural analysis of fractured basement reservoir in the South Assam Shelf, India. *Proceeding of Indian National Science Academy*, *82*(3), 923–933.

Mitra, G., Bhattacharyya, K., & Mukul, M. (2010). The Lesser Himalayan duplex in Sikkim: Implications for variations in Himalayan shortening. *Journal of Geological Society of India*, *75*, 289–301.

Mugnier, J. L., Jouanne, F., Bhattarai, R., Cortes-Aranda, J., Gajurel, A., Leturmy, P., … Vassallo, R. (2017). Segmentation of the Himalayan megathrust around the Gorkha earthquake (April 25, 2015) in Nepal. *Journal of Asian Earth Science*, *141-B*, 236–252. https://doi.org/10.1016/j.jseaes.2017.01.015ff.

Mukherjee, S. (2013). Higher Himalaya in the Bhagirathi section (NW Himalaya, India): Its structures, backthrusts and extrusion mechanism by both channel flow and critical taper mechanisms. *International Journal of Earth Science*, *102*, 1851–1870. https://doi.org/10.1007/s00531-012-0861-5.

Mukherjee, S. (2017). Review on symmetric structures in ductile shear zones. *International Journal of Earth Sciences*, *106*, 1453–1468.

Mukherjee, S., Punekar, J., Mahadani, T., & Mukherjee, R. (2015). A review on intrafolial folds and their morphologies from the detachments of the western Indian higher Himalaya. In S. Mukherjee & K. F. Mulchrone (Eds.), *Ductile shear zones: From micro- to macro-scales* (pp. 182–205). Hoboken, NJ: Wiley Blackwell.

Mukhopadhyay, B., Riguzzi, F., Mullick, M., & Sengupta, D. (2020). The strain rate and moment deficit along Indian plate boundary: A tool for estimation of earthquake hazard. *Indian Journal of Geoscience*, *74*, 1–21.

Mukhopadhyay, G., Mukhopadhyay, S. K., Roychowdhury, M., & Parui, P. K. (2010). Stratigraphic correlation between different Gondwana Basins of India. *Journal of Geological Society of India*, *76*, 251–266.

Mukhopadhyay, M. (1984a). Seismotectonics of transverse lineaments in the eastern Himalaya and its foredeep. *Tectonophysics*, *109*, 227–240.

Mukhopadhyay, S. C. (1984b). *The Tista basin: A study in fluvial geomorphology*. Kolkata: Ramkrishna Printing Works.

Naik, G. C. (2001). Sequence stratigraphy and petroleum systems of Assam shelf. ONGC. Unpublished report.

Naik, G. C., Kumar, R., & Soren, M. N. (2004). *Tectonic Setting and Petroleum System Significance of Pre-Tertiary Sediments, Assam Basin, Northeast India*. 5th Conference & Exposition on Petroleum Geophysics, Hyderabad-2004, India, (pp. 365–371).

Nandy, D. R. (2001). *Geodyanamics of Northeastern India and the adjoining region* (pp. 10–15). Kolkata: ACB Publishers.

Narayanan, K. (2005). Plate tectonics and exploration or what are the chances of finding reserves of new oil in India. In R. DSN, J. Peters, R. Shanker, & G. Kumar (Eds.), *An overview of litho-bio-chemo-sequence*,

stratigraphy and sea level changes of Indian sedimentary basins (Vol. 1, pp. 204–210). Boulder Ave. Tulsa: Association of Petroleum Geologists Sp Publication.

Nayak, B., Singh, A. K., Upadhyay, A. K., & Bhattacharyya, K. K. (2009). A note on the characters of some lower Gondwana coals of west Siang District in the Arunachal Himalaya and their trace element content. *Journal of Geological Society of India*, *74*, 395–401.

Ni, J., & Barazangi, M. (1984). Seismotectonics of the Himalayan collision zone: Geometry of the underthrusting Indian plate beneath the Himalaya. *Journal of Geophysical Research*, *89*, 1147–1163.

Pahari, S., Singh, H., Prasad, I. V. S. V., Singh, R. R., & Bhandari, A. (2008). Oil shale: An alternate source of energy and its geochemical perspective—A review. *Association of Petroleum Geologists Bulletin*, *3*, 111–117.

Pandey, M. R., Tandukar, R. P., Avouac, J. P., Vergne, J., & Heritier, T. (1999). Seismotectonics of the Nepal Himalaya from a local seismic network. *Journal of Asian Earth Sciences*, *17*, 703–712.

Panthi, A., Singh, H. N., & Shankar, D. (2013). Revisiting state of stress and geodynamic processes in Northeast India Himalaya and its adjoining region. *Geosciences*, *3*, 143–152. https://doi.org/10.5923/j.geo.20130305.01.

Patel, R. C., Singh, P., & Lal, N. (2015). Thrusting and back-thrusting as post-emplacement kinematics of the Almora klippe: Insights from low-temperature thermochronology. *Tectonophysics*, *653*, 41–51.

Pathak, M., & Kumar, S. (2019). Petrology, geochemistry and zircon U-Pb-Lu-Hf isotopes of Paleoproterozoic granite gneiss from Bomdila in the western Arunachal Himalaya, Northeast India. *Geological Society London Special Publications*, *481*(1), 341–377. https://doi.org/10.1144/SP481-2017-169.

Paul, H., Mitra, S., Bhattacharya, S. N., & Suresh, G. (2017). Active transverse faulting within underthrust Indian crust beneath the Sikkim Himalaya. *Geophysics Journal International*, *201*, 1072–1083. https://doi.org/10.1093/gji/ggv058.

Peters, J., Mahanti, S., & Singh, S. K. (2005). In R. DSN, J. Peters, R. Shanker, & G. Kumar (Eds.), *An overview of litho-bio-chemo-sequence, stratigraphy and sea level changes of Indian sedimentary basins* (Vol. 1, pp. 8–9). Boulder Ave. Tulsa: Association of Petroleum Geologists Sp Publication.

Phaye, D. K., Srivastava, D. K., Nambiar, M. V., Sinha, A. K., Prabhakar, V., & Das, S. (2013). Understanding of Petroleum Systems of Gondwana and Paleogene Sediments in Bengal Basin, India: A two (2D) dimensional basin modeling study, 10th Biennial International Conference & Exposition, Kochi, *191*, 1–8.

Potter, P. E., Franca, A. B., Spence, C. W., & Caputo, M. V. (1995). Petroleum in glacially-related sandstones of Gondwana: A review. *Journal of Petroleum Geology*, *18*, 397–420.

Pradhan, R., Prajapati, S., Chopra, S., Kumar, A., Bansal, B. K., & Reddy, C. D. (2013). Causative source of Mw 6.9 Sikkim-Nepal border earthquake of September 2011: GPS baseline observations and strain analysis. *Journal of Asian Earth Sciences*, *70*, *71*, 179–192.

Prakash, A., Singh, T., & Srivastava, S. C. (1988). Occurrence of faunal coal balls in Gondwana sediments (Permian) of Arunachal Himalaya, India. *International Journal of Coal Geology*, *9*, 305–314.

Prasad, B., Dey, A. K., Gogoi, P. K., & Maithani, A. K. (1989). Early Permian plant microfossils from the intertrappean beds of Abor Volcanics, Arunachal Pradesh, India. *Journal of the Geological Society of India*, *34*(1), 83–88.

Rajendran, K., Parameswaran, R. V., & Rajendran, C. P. (2017). Seismotectonic perspectives on the Himalayan arc and contiguous areas: Inferences from past and recent earthquakes. *Earth-Science Reviews*, *173*(3), 1–30. https://doi.org/10.1016/j.earscirev.2017.08.003.

Rajendran, K., Rajendran, C. P., Thulasiraman, N., Andrews, R., & Sherpa, N. (2011). The September 18, 2011, North Sikkim earthquake. *Current Science*, *101*, 1475–1479.

Ramachandran B., & Mallick, B. (1976). Geology of Kameng district—A review. Himalayan Geology Seminar (p. 8).

Rao, N. P., Tiwari, V. M., Kumar, M. R., Hazarika, P., Saikia, D., Chadha, R. K., & Rao, Y. B. (2015). The mw 6.9 Sikkim–Nepal earthquake of September 2011: A perspective for wrench faulting in the Himalayan thrust zone. *Natural Hazards*, *77*, 355–366.

Rattey, P. R., & Sanderson, D. J. (1982). Patterns of folding within nappe and thrust sheets: Examples from the Variscan of south-West England. *Tectonophysics*, *88*, 247–267.

Ravi Kumar, M., Hazarika, P., Prasad, G. S., Singh, A., & Saha, S. (2012). Tectonic implications of the September 2011 Sikkim earthquake and its aftershocks. *Current Science*, *102*, 788–792.

Ray, S. K. (1995). Lateral variation in geometry of thrust planes and its significance, as studied in the Shumar allochthon, Lesser Himalayas, Eastern Bhutan. *Tectonophysics*, *249*, 125–139.

Roy Chowdhury, J. (1978). Diamictites of Arunachal Pradesh. *Records of the Geological Survey of India*.

Roychowdhury, A. K., & Sinha, J. K., (1983). A report on systematic geological mapping of Gondwana rocks in Siang district, Arunachal Pradesh. Unpublished Progress Report, Geological Society of India, FS 1982–83.

Saha, D. (2013). Lesser Himalayan sequences in eastern Himalaya and theirdeformation: Implications for Paleoproterozoic tectonic activity along thenorthern margin of India. *Geoscience Frontiers*, *4*, 289–304.

Saha, D., Sengupta, D., & Das, S. (2011). Along strike variation in the Himalayan orogen and its expression along major intracontinental thrusts—The case of MCT in Sikkim and Arunachal Pradesh, India. In R. P. Tewari (Ed.), *Geodynamics, sedimentation and biotic response in the context of India-Asia collision* (Vol. 77, pp. 1–18). Bengaluru: Memoir of Geological Society of India.

Sahini, M. R., & Srivastava, J. P. (1956). Discovery of Eurydesma and Conularia in Eastern Himalaya and description of associated fauna. *Journal of the Palaeontological Society of India*, *1*, 202–214.

Sarma, J. N., & Sharma, S. (2018). Neotectonic activity of the Bomdila Fault in northeastern India from geomorphological evidences using remote sensing and GIS. *Journal of Earth System Science*, *127*, 113.

Sarma, K. P., Bhattacharyya, S., Nandy, S., Konwar, P., & Mazumdar, N. (2014). Structure, stratigraphy and magnetic susceptibility of Bomdila Gneiss, Western Arunachal Himalaya, India. *Journal of Geological Society of India*, *84*, 544–554.

Searle, M., Avouac, J. P., Elliot, J., & Dyck, B. (2017). Ductile shearing to brittle thrusting along the Nepal Himalaya: Linking Miocene channel flow and critical wedge tectonics to 25th April 2015 Gorkha earthquake. *Tectonophysics*, *714-715*, 117–124.

Sharma, S., Sarma, J. N., & Baruah, S. (2018). Dynamics of Mikir hills plateau and its vicinity: Inferences on Kopili and Bomdila Faults in Northeastern India through seismotectonics, gravity and magnetic anomalies. *Annals of Geophysics*, *61*(3), SE338. https://doi.org/10.4402/ag-7516.

Singh, A. K., Chung, S. L., & Somerville, I. D. (2022). Introduction, Part-1—Geodynamic evolution of eastern Himalaya and Indo-Myanmar orogenic belts: Advances through interdisciplinary studies. *Geological Journal*, *57*, 476–481.

Singh, A. K., & Jha, M. K. (2018). Hydrocarbon potential of permian coals of south karanpura coalfield, jharkhand, india. *Energy Sources, Part A: Recovery, Utilization, and Environmental Effects*, *40*(2), 163–171. https://doi.org/10.1080/15567036.2017.1407841

Singh, G. (1983). On the field disposition of Gondwanas in part of Kameng an Subansiri districts, Arunachal Pradesh. *Geological Survey of India, Miscellaneous Publication*, *43*, 128–133.

Singh, K., & Thakur, V. C. (2001). Microstructures and strain variation across the footwall of the Main Central Thrust Zone, Garhwal Himalaya, India. *Journal of Asian Earth Sciences*, *19*, 17–29.

Singh, M. P., & Singh, P. K. (1994). Indications of hydrocarbon generation in the coal deposits of the rajmahal basin, bihar: revelations of fluorescence microscopy, *Journal of Geological Society of India*, *43*, 647–658.

Singh, P., & Patel, R. C. (2017). Post-emplacement exhumation history of Almora klippe of Kumaun-Garhwal Himalaya, NW-India as revealed by fission track thermochronology. *International Journal of Earth Sciences*, *106*, 2189–2202.

Singh, P., & Patel, R. C. (2022). Miocene development of MBT, Ramgarh Thrust and exhumation of lesser Himalayan rocks of Kumaun-Garhwal region, NW-Himalaya (India): Insights from fission track thermochronology. *Journal of Asian Earth Sciences*, *224*, 104987.

Singh, P., Patel, R. C., & Chaudhary, S. K. (2022). Fission track thermochronology basic fundaments, technique and its geological application: A case study from Kumaun-Garhwal Himalaya. *Himalayan Geology*, *43*(1A), 96–110.

Singh, P., Patel, R. C., & Lal, N. (2012). Plio-Pleistocene in-sequence thrust propagation along the Main Central Thrust zone (Kumaon-Garhwal Himalaya, India): New thermochronological data. *Tectonophysics*, *574-575*, 193–203. https://doi.org/10.1016/j.tecto.2012.08.015.

Singh, P., Sethy, P. C., Rastogi, H., Singh, M. R., Singh, A. K., Thakur, S. S., & Singhal, S. (2022). Geological field observations along the Pandoh Syncline: The Mandi-Kataula-Bajaura section of Himachal Pradesh, NW-India. In S. Mukherjee (Ed.), *Structural geology & tectonics field guidebook* (Vol. 2), Singapore.

Singh, P., Singhal, S., & Das, A. N. (2020). U-Pb (zircon) geochronology of the Chaur granitoids, Jutogh Group of Himachal Himalaya, NW-India: Significance of the Neoproterozoic magmatism related to Grenvillian orogeny and assembly of the Rodinia supercontinent. *International Journal of Earth Sciences*, *109*(1), 373–390.

Singh, S., & Chowdhury, P. K. (1990). An outline of the geological framework of the Arunachal Himalaya. *Himalayan Geology*, *1*, 189–197.

Singh, T. (1973). Note on Upper Palaeozoic fauna from Subansiri district, Arunachal Pradesh. *Himalayan Geology*, *3*, 401–410.

Singh, T. (1975). *Discovery of Eurydesma of Siang district Arunachal Pradesh* (pp. 90–91). VIII: Bulletin of Indian Geological Association.

Singh, T. (1979). Palynostratigraphy of the Permian rocks of Siang district, Arunachal Pradesh. In *Metamorphic rock sequences of the Eastern Himalaya* (pp. 191–194). Washington D.C: American Geophysical Union.

Singh, T. (1987). Permian biogeography of the Indian subcontinent with special reference to the marine fauna. In I. Mackenzic & D. Garry (Eds.), *Gondwana 6, Geophysical monograph* (Vol. 41, pp. 141–194). Washington, DC: American Geophysical Union.

Singh, T. (2013). Mineral resource potential of Arunachal Pradesh and its socio-economic importance, Journal of Indian Geological Congress, 18th Convention Special Volume (pp. 103–113).

Singh, T., & Mathur, A. K. (1982). Description of Eurydesma and associated fauna from Subansiri. *Record of Geological Survey of India*, *11*(4), 53–57.

Singh, T., & Singh, P. (1983). Late Early Eocene larger foraminiferids from Siang district, Arunachal Pradesh, India and their geological significance. *Geoscience Journal*, *IV*, *2*, 141–156.

Sinha, N. K., & Mathur, A. K. (1977). *Stratigraphy and structure of Gondwana of Arunachal Pradesh*. Unpublished Progress Report, Geological Survey of India, FS 1976–77.

Sinha, N. K., & Mishra, U. K.(1984). Geological survey of India, *NER News*, *6* (1).

Sinha, N. K., Satsangi, P. P., & Mishra, U. K. (1986). Palaentology of Permian and Eocene rocks of Siang district, Arunachal Pradesh. *Record of the Geological Survey of India*, *114*(iv), 51–60.

Srinivasan, V. (2003). Stratigraphy and structure of Siwaliks of Arunachal Pradesh: A reappraisal through remote sensing techniques. *Journal Geological Society of India*, *62*, 139–151.

Srivastava, H. B., Srivastava, V., Srivastava, R. K., & Singh, C. K. (2011). Structural analyses of the crystalline rocks between Dirang and Tawang, west KamengDistrict, Arunachal Himalaya. *Journal of the Geological Society of India*, *78*, 45–56.

Srivastava, S. C., & BhattAcharya, A. P. (1996). *Palynological assemblage from Permain sediments, West Siang distrct, Arunachal Pradesh*. Gondwana nine Pt. I, Proceedings of 9th Indian Gondwana Group, Hyderabad, India (pp. 261–268).

Thomas, W. A. (2006). Tectonic inheritance at a continental margin. *GSA Today*, *16*, 4–11.

Tiwari, R., & Srivastava, A. K. (2000). Plant fossils from Bhareli Formation of Arunachal Pradesh. *North-East Himalaya, India Palaeobotanist*, *49*, 209–217.

Tripathi, C., & Roy Chowdhury, J. (1983). Gondwana of Arunachal Himalaya. *Himalayan Geology*, *11*, 73–89.

Trouw, R. A. J., Tavares, F. M., & Robyr, M. (2008). Rotated garnets: A mechanism to explain the high frequency of inclusion trail curvature angles around 90° and 180°. *Journal of Structural Geology*, *30*(8), 1024–1033. https://doi.org/10.1016/j.jsg.2008.04.011.

Verma, P. K., & Tandon, S. K. (1976). Geologic observation in a part of the Kameng district, Arunachal Pradesh (NEFA). *Himalayan Geology*, *6*, 259–286.

Verma, R. K. (1985). *Gravity field, seismicity and tectonics of the Indian peninsula and the Himalaya* (Vol. 184). Dordrecht: D Reidel Publishing Company.

Verma, R. K., & Mukhopadhyay, M. (1977). An analysis of the gravity field in northeastern India. *Tectonophysics*, *42*, 283–317.

Wojtal, S., & Mitra, G. (1988). Nature of deformation in fault rocks from Appalachian thrusts. In G. Mitra & S. Wojtal (Eds.), *Geometry and mechanisms of thrusting with special reference to the Appalachians* (Vol. 222, pp. 17–34). Boulder, Co: Geological Society of America Special Paper.

Yin, A. (2006). Cenozoic tectonic evolution of the Himalayan orogeny as constrained by along strike variation of structural geometry, exhumation history, and foreland sedimentation. *Earth-Science Reviews*, *76*, 1–131.

Yin, A., Dubey, C. S., Webb, A. A. G., Kelty, T. K., Grove, M., Gehrels, G. E., & Burgess, W. P. (2010a). Geological correlation of the Himalayan orogen and Indian craton: Part 1. Structural geology, U-Pb zircon geochronology, and tectonic evolution of the Shillong Plateau and its neighboring regions in NE India. *Geological Society of America Bulletin*, *122*, 336–359.

Yin, A., Dubey, C. S., Webb, A. A. G., Kelty, T. K., Grove, M., Gehrels, G. E., & Burgess, W. P. (2010b). Geologic correlation of the Himalayan orogen and Indian craton: Part 2. Structural geology, geochronology and tectonic evolution of the Eastern Himalaya. *Geological Society of America Bulletin*, *122*, 360–395.

Yin, A., & Harrison, T. M. (2000). Geologic evolution of the Himalayan–Tibetan orogen. *Annual Review of Earth and Planetary Sciences*, *28*, 211–280.

Zhang, Z., Xiang, H., Dong, X., Ding, H., & He, Z. (2015). Long-lived high-temperature granulite-facies metamorphism in the Eastern Himalayan orogen, South Tibet. *Lithos*, *212-215*, 1–15.

Zhao, Y., Grujic, D., Baruah, S., Drukpa, D., Elkadi, J., Hetenyi, G., … Welte, C. (2021). Paleoseismological findings at a NewTrench indicate the 1714 M8.1 earthquake ruptured the Main frontal thrust over all the Bhutan Himalaya. *Frontiers in Earth Science*, *9*, 689457. https://doi.org/10.3389/feart.2021.68945.

SUPPORTING INFORMATION

Additional supporting information may be found in the online version of the article at the publisher's website.

How to cite this article: Goswami, T. K., Kalita, P., Mukherjee, S., Mahanta, B. N., Sarmah, R. K., Laishram, R., Saikia, H., Gogoi, M., Machahary, R., & Oza, B. (2022). Basement cross-strike Bomdila Fault beneath Arunachal Himalaya: Deformation along curved thrust traces, seismicity, and implications in hydrocarbon prospect of the Gondwana sediments. *Geological Journal*, *57*(12), 4974–4999. https://doi.org/10.1002/gj.4514